University of Louisville

ThinkIR: The University of Louisville's Institutional Repository

Electronic Theses and Dissertations

12-2017

Deficiency of RDH10 causes cleft secondary palate in mouse.

Swetha Raja
University of Louisville

Recommended Citation

Raja, Swetha, "Deficiency of RDH10 causes cleft secondary palate in mouse." (2017). *Electronic Theses and Dissertations.* Paper 2852.
https://doi.org/10.18297/etd/2852

DEFICIENCY OF RDH10 CAUSES CLEFT SECONDARY PALATE IN MOUSE

By Swetha Raja

A Thesis

Submitted to the Faculty of the

School of Dentistry at the University of Louisville

In Partial Fulfillment of the Requirements

For the Degree of

Master of Science in Oral Biology

Department of Oral Immunology and Infectious Diseases

University of Louisville

Louisville, Kentucky

December 2017

DEFICIENCY OF RDH10 CAUSES CLEFT SECONDARY PALATE IN MOUSE

By

Swetha Raja

Bachelor of Dental Surgery.

Sri Ramachandra University, 2015

Thesis Approved on

November 9, 2017

By the following Thesis Committee:

_____

Dr. Lisa Sandell. Ph. D.

_____

Dr. Shuang Liang, Ph.D.

_____

Dr. Jiaxing Ding, Ph.D.

_____

Dr. Mark Running, Ph.D.

_____

DEDICATION

This thesis is dedicated to my father Raja, mother Uma

brother Santosh and my husband Sundaram

who have been my constant guidance and pillars of support.

I could not have done it without them and I owe this work to them.

ACKNOWLEDGEMENTS:

ABSTRACT:

DEFICIENCY OF RDH10 CAUSES CLEFT SECONDARY PALATE IN MOUSE

Swetha Raja

November 9, 2017

The focus of this project is to understand the role of Retinoic Acid (RA) produced by RDH10-mediated metabolism of Vitamin A in palate development. For 80 years now, we have known that dietary restriction of RA/Vitamin A can cause cleft palate but we have failed to understand how RA deficiency causes cleft palate. Our gap in knowledge about how RA deficiency causes cleft palate is mainly owing to the fact that we lack a model system to study such defects. The aim of this thesis research project was to determine if conditional inactivation of the Vitamin A metabolic gene *Rdh10* in mouse could serve as an experimental model system to study the etiology of RA deficient cleft palate in mammals. This study examined a mouse model system in which *Rdh10* was conditionally inactivated using a Tamoxifen-inducible cre-lox system.   At embryonic age 16.5 (E16.5), when palate fusion was complete in control embryos, we observed 44% of the *Rdh10* conditional mutant embryos had complete cleft of the secondary palate. Histological analysis at E12.5 revealed defects in palate shelf morphology in mutant embryos. Defects at this stage included reduced palate shelf outgrowth and a lack of groove between the shelf and the body of the maxilla. We used a

v

BrdU assay to label proliferating cells, and identified an increase in cell proliferation at the bend region in the mutant embryos compared to controls. Using a reporter mouse strain to detect RA signaling we observed RA signaling within the anterior palate shelf tissues. In order to understand if the cleft palate seen in *Rdh10* mutant embryos was due to defects intrinsic to the palate or if the clefts were secondary to abnormalities in development of the mandible or tongue, we isolated and cultured maxilla from control and mutant embryos. We observed that there was no significant difference in fusion rate of palate shelves between control and mutant maxillae cultured *ex vivo*. In summary, these data demonstrate conditional inactivation of *Rdh10* in mice proves to be an effective experimental model system to study how deficiency of RA causes cleft palate. Our findings indicate that RA signaling is active in palate tissue and regulates cell proliferation and palate shelf morphology. However, we find that the primary defect causing cleft palate in RA deficient embryos is not intrinsic to the maxilla. This study opens the door for future investigation to how RA deficiency cause cleft palate by mechanisms extrinsic to the maxilla.

TABLE OF CONTENTS

LIST OF FIGURES

LIST OF TABLES

CHAPTER 1: INTRODUCTION AND BACKGROUND

1.1 Palate Overview:

In humans and other mammals, the palate forms a mechanical barrier that anatomically separates the oral cavity from the nasal cavity. This enables proper breathing and food intake essential for survival. It also plays an important role in speech and articulation. Structurally, the palate is formed from two distinct components, the primary and the secondary palate. The part of the palate that is present anterior to the incisive foramen is the primary palate and the part that is present posterior to the incisive foramen is the secondary palate (Fig 1). Embryologically, the primary palate is formed from the frontonasal prominence. The secondary palate develops from the palatal shelves that arise as medial outgrowths of the maxillary process. The secondary palate is structurally composed of the hard palate and the muscular soft palate.

The development of palate is well regulated by genetic and environmental factors. Any disturbance during the development process of the palate can result in a major congenital birth defect called cleft palate. This is discussed in the next section.
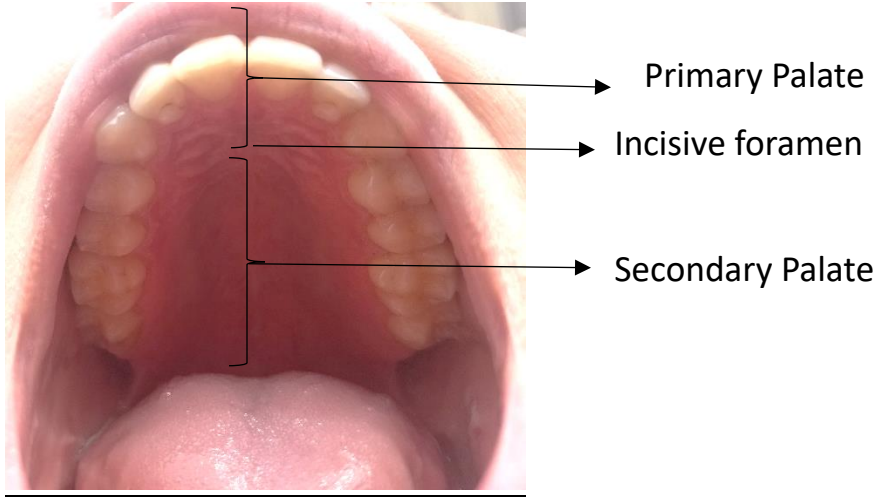
Figure 1. Schematic representation of the definitive palate

1.2 Congenital Birth Defects:

Congenital anomalies, also known as birth defects, are anatomical abnormalities that occur during the development of a fetus. One in every 33 child born each day suffer from a congenital defect, which approximates to 120000 babies each year. One in five children die of birth defects. Even infants who survive birth defects often face physical, social and psychological challenges (Centers for Disease Control and Prevention [CDC] 2014).

One of the most common craniofacial birth defect known in humans are orofacial clefts (Canfield, Honein et al. 2006). Although the incidence of orofacial clefts varies across different geographic areas and ethnic groups, one child in every 700 suffers from some form of orofacial cleft. Orofacial cleft is a broad terminology that includes complete midline cleft, cleft lip with or without cleft palate, and cleft of the secondary palate.

We have several systems of classification of orofacial clefts. The one most commonly used in clinical scenario is the Veau system. The Veau system classifies orofacial cleft into 4 groups based on whether the primary and/or secondary palates are affected (Veau V. Division Palatine. 1931) (Table 1).

For research purposes, we can classify orofacial clefts as syndromic or non-syndromic clefts. This helps us better understand the functions of genes and other factors in the development of craniofacial structures and other organs. Although the majority of cleft lip and palate cases are non-syndromic, cleft lip and palate have also been reported as a feature of over 300 syndromes.(Marazita 2002). It is

valuable to note that cleft palate has been associated with Pierre Robin Syndrome (PRS). PRS is characterized clinically by micrognathia, cleft palate and early respiratory difficulty caused by glossoptosis. Mouse model of PRS has been implicated in several gene mutations such as *Sox-9, Sox-11*(Benko, Fantes et al. 2009, Huang, Yang et al. 2016).

Cleft palate poses severe functional limitations, expensive health care cost and serious pyscho-social disturbance to children suffering with this defect. Although we have improved treatment options available to treat cleft palate, our aim as a researcher is to understand how the palate develops and how its development and this information can be applied to prevent cleft palate occurrence in the future. One of the commonly used tools in developmental biology to understand morphogenesis and development is the mouse embryonic model. The mouse model closely simulates the development of palate in human embryos. The development of palate in mouse is reviewed in detail in the next section.

Veau Classification of Cleft Palate

Class I	Incomplete cleft, soft palate only (no unilateral/ bilateral designation)
Class II	Hard and soft palate, secondary palate only (No unilateral/bilateral designation)
Class III	Complete unilateral cleft including lip (Primary and secondary palates)
Class IV	Complete bilateral cleft

Table 1. Classification of cleft palate- The Veau System

1.3 Development of Palate in Mouse:

The development of the secondary palate is a multi-step process that involves cell migration, cell differentiation, proliferation, and apoptosis. In mouse embryos, the development of the secondary palate can be divided into stages of initiation, vertical growth, medial growth and fusion (Bush and Jiang 2012).

The craniopharyngeal ectoderm and the migratory mesenchymal neural crest cells together give rise to the maxillary processes(Ferguson 1988). The mouse palate developmental stages mentioned above begin at embryonic stage 10.5 (E10.5), identical to the sixth developmental week in humans. At embryonic stage E10.5, the bilateral maxillary processes begin to fuse with the medial nasal process to give rise to the upper lip and the primary palate (Gritli-Linde 2007). The development of the secondary palate begins by E11.5, whereby the growth of the palatal shelves is initiated as medial outgrowths of the maxillary processes.(Bush and Jiang 2012). This stage is called initiation. The palatal outgrowths then grow vertically on either side of the tongue. The next step in palate development is elevation. Two models have been proposed as mechanisms for palate elevation. The early model suggest that the palatal shelves elevate by a rotating mechanism at E14.0 (Ferguson 1988, Gritli-Linde 2007). However, a recent model of palate development is gaining popularity. Current understanding of literature says that the elevation of palate shelf is rather more complicated than a simple flip up mechanism that was widely accepted before. The horizontal palate shelf is formed as an outgrowth from the side of the vertical palate shelf rather than the rotation mechanism (Jin, Tan et al. 2010). After palate shelves are horizontally placed, they

6

grow medially towards the midline and the two palatal shelves on either side contact in the midline at E14.5. The anteromedial boundary of the palatal shelves fuses with the primary palate. The upper border of the palatal shelves fuse with the inferior border of the nasal septum (Kauffman 1992).The medial epithelium seam disintegrates (Gritli-Linde 2007), leading to mesenchymal interaction and fusion of the palatal shelves.

Even though, the different steps of palate development were established as early as 1924 (Peter 1924), the regulation of these events and the etiology underlying cleft palate is still not well understood. The development of the palate is not as simple as it seems, but rather complex. It is tightly regulated by genetic and environmental factors. The genes and the environmental factors further cause intrinsic disruptions within the palate shelf tissues or extrinsic disruptions to surrounding orofacial structures, resulting in cleft palate(Ferguson 1988).

DEVELOPMENT OF THE SECONDARY PALATE-MOUSE
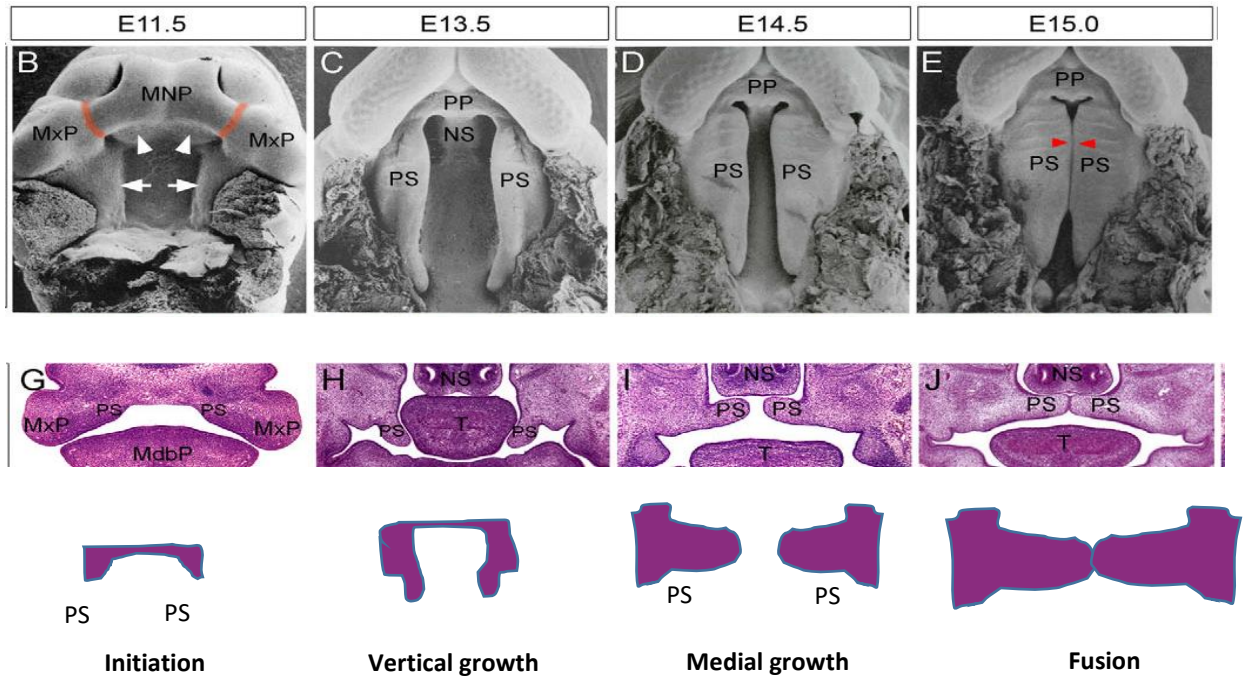
Adapted from **2012, Jeffrey O. Bush and Rulang Jiang**

(Used with Permission)

Figure 2. Development of the secondary palate in mouse.

1.4 Factors Causing Cleft Palate

1.4.1 Cleft palate caused by intrinsic or extrinsic defects

Cleft palate can occur as a result of defects that occur within the palate shelf tissues directly, or by abnormalities of the tongue or mandible that hinder palate shelf elevation. Disturbances that occur within the palate shelf tissue directly are known as "intrinsic" defects. Disturbances that result from primary defects in the tongue or mandible that secondarily result in cleft palate are known as "extrinsic" defects.

Intrinsic disruptions can affect the initiation, growth, elevation and/or fusion of the palate shelf tissue. These disruptions can be caused by both genetic and environmental factors.

Extrinsic disruptions can result from abnormalities of the tongue or mandible that physically impede the elevation of the palate shelves. During normal palate development, the descent of the tongue and growth of the mandible downward happens prior to palate shelf elevation. If the mandible fails to grow to make room for descent of the tongue, or if the tongue fails to withdraw due to defects in myogenesis, then palate shelf elevation can be blocked and cleft palate can occur. It has been published in the literature that mouse mutations in *Sox9* or *Hoxa2* lead to cleft palate due to defective mandibular development, or defects in tongue myogenesis, respectively (Gendron-Maguire, Mallo et al. 1993, Bi, Huang et al. 2001, Mori-Akiyama, Akiyama et al. 2003).

1.4.2 Cleft palate caused by genetic or environmental factors:

Disturbances in genetic and environmental factors that control palate development can cause cleft palate.

Gene mutations in transcription factors, growth factors and signaling molecules have been implicated in cleft palate (Rice, Spencer-Dene et al. 2004, Alappat, and Zhang et al. 2005). Signaling molecules, such as sonic hedgehog (SHH), transforming growth factors (TGF), and fibroblast growth factors (FGF) have been shown to be involved in palate development. Alterations and gene mutations in these factors have been implicated in cleft palate in mice (Table 2).

In addition to genetic influence on palate development, environmental factors can also cause cleft palate. Maternal diet or nutrition are known environmental factors that are linked to palate formation. During the development of the fetus, the nutritional status of the embryo is dependent on maternal diet, intake, and metabolism of food. Maternal diet is crucial particularly during the first trimester when major organs such as brain and heart develop. Both excess and deficiency of a nutrient could cause craniofacial anomaly. Amongst all nutrients, vitamins are of particular importance, as they cannot be synthesized within the body. Vitamins play a crucial role during growth and development and hence are considered as a vital ingredient of embryonic nutrition. For example, folate deficiency in the mother can cause neural tube defects and cleft palate in offspring (Wilcox, Lie et al. 2007).

Gene Mutation	Intrinsic/ Extrinsic Defect	Reference Paper
Tgfβ3	Intrinsic defective in proliferation. Primary defect in fusion of palatal shelves.	(Kaartinen, Voncken et al. 1995, Proetzel, Pawlowski et al. 1995).
Cyp26b1	Intrinsic- Defective regulation of *fgf10*	(Okano, Kimura et al. 2012)
Fgf10	Proliferation defect; Increased Apoptosis; Defective adhesion to other structures.	(Rice, Spencer-Dene et al. 2004, Alappat, Zhang et al. 2005)
Pdgfc	Intrinsic: Hypoplasia of Palate Shelves with vertically oriented palate shelves.	(Ding, Wu et al. 2004)
Shh	Defect in proliferation and apoptosis	(Rice, Spencer-Dene et al. 2004)

Table 2. Genes implicated in cleft palate in mice.

1.5 Vitamin A Metabolism:

Vitamin A is a small lipid soluble molecule that forms one of the most essential maternal nutrients. Liver, carrots and other green leafy vegetables have good amounts of Vitamin A. Retinoic acid (RA) is the biologically active form of Vitamin A. RA regulates many aspects of embryogenesis (Clagett-Dame and Knutson 2011). Hence, knowledge about metabolism of Vitamin A into active RA, and how RA regulates embryonic morphogenesis of specific tissues, are needed for establishing a fundamental understanding in developmental biology. This understanding will prove to be beneficial for future prevention of disease and its progression.

Vitamin A is converted into RA by a series of enzymatic reactions. The first step in this process involves the conversion of retinol into intermediate product, retinal. This conversion is done by two groups of enzymes, the alcohol dehydrogenase family (ADH) and the short chain dehydrogenase/ reductase family (SDR). For a very long time, due to ubiquitous expression pattern of the ADH family and inadequate study techniques, the conversion of retinol to retinal was considered in essential for embryogenesis. Recently, RDH10 has been shown to be a critical enzyme in the metabolism of Vitamin A into RA (Sandell, Sanderson et al. 2007, Sandell, Lynn et al. 2012). Mutants that lack RDH10 cannot metabolize Vitamin A and show drastic deficiency in production of RA that affects embryogenesis(Metzler and Sandell 2016). Generally, mutants that show complete knockout of *Rdh10* die as early as E11.5.

RA has been known to be regulator of proliferation, differentiation, and apoptosis of cells and has a known role in regulating gene expression (Rhinn and Dolle 2012). RA regulates gene expression by activating nuclear receptors of the retinoic acid receptors (RAR) that bind to regulatory DNA elements of target genes (RA Response Elements) (Fig 3).

The regulation of endogenous levels of RA is critical for embryo development. Both excess RA and insufficient RA result in craniofacial malformations. The effects of excessive RA have been well studied using mice lacking cytochrome P450 enzymes, which control RA levels by degrading RA, and by supplementation of excess RA in maternal diet (Abu-Abed, Dolle et al. 2001, Sakai, Tokunaga et al. 2001, Okano, Kimura et al. 2012). In contrast, the effects of reduction in normal endogenous levels of RA is incompletely understood and there are no published articles put forth so far on this important topic.

Vitamin A is converted into active form RA

H₃C CH₃ all–*trans*–Retinol
H₂OH (Vitamin A)
CH₃

RDH10

H₃C CH₃ all–*trans*–Retinal
C=O
CH₃

H₃C CH₃ Retinoic Acid
COOH
CH₃

RAR RXR

Developmental genes
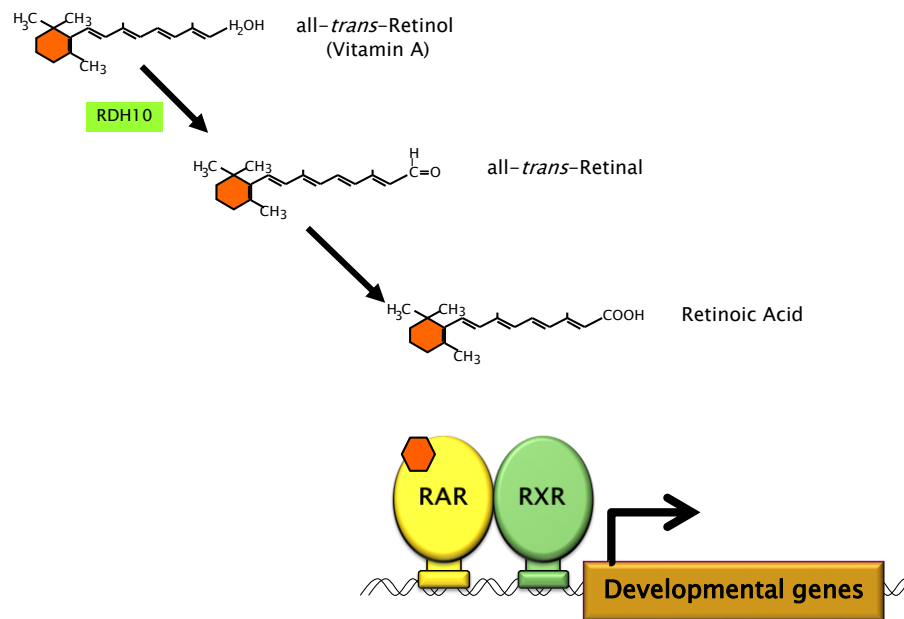
Sandell Lab

Figure3.Vitamin A Metabolism. This figure demonstrates the enzymatic conversion of Vitamin A into RA. The first step in this process involves one of the key enzymes in this regulatory pathway, RDH10. RDH10 aids in oxidation of retinol into its intermediate, retinal. The next step is the conversion of retinal into RA. RA is the active metabolite of Vitamin A and regulates transcription of developmental genes, cell differentiation, proliferation, and apoptosis.

1.6 Perturbations of Vitamin A are Associated with Cleft Palate in Humans

In addition to mouse studies, Vitamin A deficiency or excess has been shown to be associated with increased incidence of cleft palate in humans. Epidemiological studies have revealed that maternal diets that are low in Vitamin A show higher correlation with incidence of orofacial clefts (Krapels, van Rooij et al. 2004). Interestingly, dietary intake of rich sources vitamin A, for example liver, reduce the risk of cleft (McKinney, Chowchuen et al. 2013). Children born with clefts also have reduced serum vitamin A levels (Zhang, Zhou et al. 2014). On the other hand, increased consumption of Vitamin A or RA supplements have also shown to be associated with orofacial clefts (McKinney, Chowchuen et al. 2013) (Krapels, van Rooij et al. 2004).

In summary, both excess and reduced maternal levels of Vitamin A causes cleft palate in offspring. Since RA signaling is regulated by the metabolism of a nutrient in the diet, we can intervene this signaling pathway for the purpose of prevention of cleft palate. The study and understanding of how vitamin A metabolism can be intervened to provide therapeutic benefits can be done in animal models and the results may be applied to the prevention of occurrence of cleft palates in humans.

1.7 Focus of My Thesis Project:

Because Vitamin A and its metabolic products have the potential to influence the incidence of orofacial clefts, it is important to understand how vitamin A metabolism and RA signaling regulate the development of the secondary palate. Although the teratogenic effects of excessive intake of RA have been explored, we have not been able to understand the role of deficient RA in the development of cleft palate for over 80 years now due to technical difficulties. Dietary models of Vitamin A/RA deficiency affect the health of the mother. Complete knock out model of various enzymes that aid in the metabolism of Vitamin A have early embryonic death even before the initiation of palate development (Lohnes, Mark et al. 1994, Halilagic, Ribes et al. 2007). Adding on to the above reasons, we have also not been to understand the functions of enzymes that aid in the metabolism of Vitamin A until very recently (Sandell, Sanderson et al. 2007). Hence, to date the effects of reduced RA in the development of palate remains an unexplored territory in developmental biology.

To resolve this issue and to understand the role of endogenous RA in the development of palate, my project at the Sandell lab utilizes a genetic model that will allow us to cause RA deficiency in a stage specific manner by conditional inactivation of RDH10, a critical enzyme that catalyzes the first step in the conversion of Vitamin A into RA. Other lab members have investigated the efficiency of tamoxifen induced excision of *Rdh10*. *Rdh10* is excised effectively within 48 hours after administration of tamoxifen at either embryological age E7.5 or E8.5.

16

Using this model system, I would like to answer the following questions:

1. Is *Rdh10* required for development of the secondary palate?

2. Does RA signaling occur in the palate?

3. Does RA produced by *Rdh10* regulate cell proliferation in the developing palatal mesenchyme?

4. If *Rdh10* inactivation causes cleft palate, is the defect due to intrinsic mechanism within the palate shelves or extrinsic mechanism due to abnormality of the tongue or mandible?

My thesis focuses on answering these key questions on the role of endogenous RA during development of palate.

Over the course of this study, I have identified that conditional inactivation of *Rdh10* is an effective model system to study the effects of RA deficiency in development of cleft secondary palate. I show that conditional inactivation of *Rdh10* causes cleft palate in mutant embryos. I show that administration of tamoxifen at different gestational stages yields different percentages of cleft palate, indicating that *Rdh10* function is required at a specific stage of palate development. I have demonstrated the presence of RA signaling in the palate at E12.5. In addition, I demonstrate that RDH10/RA deficient palates cultured ex vivo without the mandible and tongue fuse at the same rate as controls, suggesting that the primary defect in these mutants is extrinsic to the palate shelves.

CHAPTER 2: MATERIALS AND METHODS

2.1 Animals:

All experiments involving mice were performed in accordance to the protocol that was approved by the institutional animal care and use committee (IACUC) at the University of Louisville. The approval number for the same is #15190. The day of vaginal plug was considered E 0.5.

The RARE-Lac Z reporter mouse was used to understand the spatiotemporal distribution of RA within the palate shelves. These reporter mice were obtained from Jackson Laboratories (Official Name: Tg (RARE-Hspa1b/ lacZ) 12Jrt).

The *Rdh10 flox/flox* ER^{T2} Cre mice B6.129-Gt(ROSA)26Sor tm1(cre/ER^{T2}) Tyj/J were obtained from the Jackson laboratory (Strain 008463). The *Rdh10*+/- mice lines used in this study were generated and maintained as described previously by (Sandell, Sanderson et al. 2007, Sandell, Lynn et al. 2012).

2.2 Generation of *Rdh10* Conditional Mutants

In order to create a timed inactivation of the *Rdh10* gene, we crossed *Rdh10$^{flox/flox}$* Er^{t2}Cre2$^{+/+}$ with *Rdh10$^{+/-}$*. This cross produces embryos of two different genotypes, heterozygous *Rdh10$^{flox/+}$* Ert2Cre embryos, which have one wild type copy of *Rdh10* and serve as controls, and *Rdh10$^{flox/-}$* Ert2Cre, which become *Rdh10$^{-/-}$* mutant upon exposure to tamoxifen.

Mutant mice experience *Rdh10* inactivation upon activation of the Cre recombinase enzyme. Activation of the Cre recombinase was done by administration of single dose of Tamoxifen at either E7.5, or E8.5, or E9.5, or E10.5.

After administration of tamoxifen, pregnant mice were euthanized at E16.5 using carbon dioxide gas. Following this euthanasia, cervical dislocation was also performed to verify that that the animal was deceased before we began dissection. Embryos were harvested and decapitated from the body. Harvested embryos were transferred to vials containing10Mm PBS (phosphate buffered saline). The vials were individually labelled and the tails were sent for genotyping. Embryo heads were fixed in 4% paraformaldehyde (PFA) at 4^0C for 24-48 hours and then transferred back to PBS.

For understanding mechanistic role of *Rdh10* deficient cleft palate Embryos were harvested at various palate developmental stages (E12.5, E13.5, E14.5, and E15.5 & E16.5) after administration of tamoxifen at E8.5.

We administered 5mg Tamoxifen and 1 mg progesterone in 250 µL of corn oil by oral gavage to individual pregnant female mice after successful mating. This amount of tamoxifen and progesterone was determined empirically.

2.3 Stain for RARE-Lac Z Reporter Activity:

RARE-LAC Z reporter mice were used to show RA signaling in the developing palate shelves. RARE-lacZ activity was assayed by X-gal staining. For the staining, we fixed whole embryo or tissue specimens in 2% Paraformaldehyde and 0.2%

glutaraldehyde for 60 min on ice. Following fixation, specimens were rinsed and incubated in Rinse A solution for 30 min at room temperature. The composition of Rinse A solution is 5 mM EGTA/2 mM MgCl2/PBS pH 7.3 that was either lab mixed or purchased from Millipore. Specimens were then rinsed and incubated in pre warmed Rinse B for 15 minutes at 37 °C. Rinse B solution composed of 2 mM MgCl$_2$/0.01% Sodium deoxycholate/0.02% NP40/PBS pH 7.3 that was either lab mixed or obtained from Millipore. When specimens were fixed, rinsed, and ready to be stained, X-gal (Sigma-Aldrich B4252, suspended at 40 mg/ml in Dimethyl Formamide) was added to Stain Base Solution to a final concentration of 1 mg/ml. Specimens were incubated in stain solution overnight at 37 °C in the dark. After staining, specimens were post-fixed in 4% Paraformaldehyde overnight at 4 °C. For section staining of RARE lacZ embryos, stained whole mount specimens were equilibrated to paraffin using minimal incubation times in neo-clear xylene substitute and embedded. After sectioning, slides were de-paraffinized and counterstained briefly with Nuclear Fast Red.

2.4 Whole Mount Nuclear Fluorescent Imaging:

To analyze morphology of the palate tissue, embryos were collected at embryonic stage E16.5 and the mandibles were dissected away to aid in visualizing the palate shelves. Embryo morphology was visualized by staining whole embryos with DAPI to label all cell nuclei and imaging fluorescent signal. Embryos were fixed in 4% formalin overnight at 4°C and then stained with 2 µg/ml DAPI in PBS, a protocol previously described in (Sandell, Kurosaka et al. 2012). Imaging of these embryos was done using the Leica M165FC Microscope.

2.5 Fixation and paraffin embedding of samples:

In order to do Hematoxylin and Eosin staining for morphological analysis and Brdu assay for proliferation, embryo samples were harvested at different stages of palate development. Head samples were fixed in 4% Paraformaldehyde (PFA) at 4°C on a shaker for 24-48 hours (depending on the age of the embryo). Samples were then washed in PBS briefly. Samples were then dehydrated through a series of graded ethanol (EtOH) (IBI Scientific, Biotechnology grade) at room temperature with shaking in the following sequence: washed in 25% EtOH for 30 minutes, then 50% EtOH for 30 minutes, then 70% EtOH for 30 minutes once. The 70% EtOH solution was changed and embryos were left in the solution overnight. Following that, samples were then washed in 95% EtOH for 30 minutes once, then 100% EtOH for 30 minutes two times. Following ethanol dehydration, the samples were washed in neoclear: ethanol mixture at 1:1 ratio for 30 minutes on a rocking platform at room temperature. Samples were then immersed in neoclear for 15 minutes twice. Then, samples were immersed in tissue embedding medium (Paraplast Xtra, McCormick Scientific) for 45 minutes. The paraffin was changed after 45 minutes and samples were placed in a vacuum chamber for another 45 minutes. Finally, fixed mouse heads were embedded in an embedding block with paraffin wax. Serial frontal sections 8µm thick were prepared using the microtome (Microm HM315).

2.6 Histological Analysis:

For histological analysis, embryos were dissected at desired stages from timed pregnant mice, fixed in 4% paraformaldehyde (PFA), dehydrated through an

ethanol series, embedded in paraffin as mentioned in the previous section. Before proceeding to the staining protocol, samples were first deparaffinized in the oven at 58°C for 30 min. Following deparaffinization, the samples were then rehydrated through xylene (Fisher Scientific, Waltham, Massachusetts, USA) and a graded ethanol series (EtOH) (IBI Scientific, Biotechnology grade) at room temperature in the following sequence: immerse the slides in xylene for 10 minutes twice, then 100% EtOH for 10 minutes twice, then 95% EtOH for 2 minute once, then 70% EtOH for 2 minutes once, and finally in PBS for 1 minute twice. Next, slides were immersed in hematoxylin stain (Modified Harris Hematoxylin, Sigma-54 Aldrich, St. Louis, MO, USA) for 8 minutes. The slides were then placed under running water for 5 minutes, following which they were transferred to acid alcohol for 30 seconds. The slides were once again shown in running tap water for 2 minutes and then transferred to lithium carbonate for 45 seconds. The slides were washed again in running tap water for 5 minutes. Next, the slides were dipped in 80% EtoH 10 times and then stained with eosin for 40 seconds. Slides were dehydrated through graded ethanol (EtOH) series and xylene at room temperature in a fume hood in the following sequence: then 95% EtOH for 5 minutes, then 100% EtOH for 10 minutes twice, then Xylene for 10 minutes and then in a new xylene for 10 minutes. After that sufficient amount of xylene based permount media was placed on each slide, and a coverslip was mounted. The slides were then viewed using the Axiocam MRC5 microscope.

<u>2.7 BrdU Assay</u>

To understand mechanistic role of RA deficiency in cleft palate, we analyzed cell proliferation by BrdU incorporation, pregnant females at E12.5 were injected BrdU (100mg/kg, Sigma Aldrich) intraperitoneally. After 3 Hours, the embryos were harvested, decapitated and the heads were fixed in 4% PFA for 24 hours. The heads were then dehydrated through series of ethanol changes and embedded in paraffin for sectioning by routine procedures. For BrdU assay, these sections were deparaffinized and rehydrated through series of ethanol and PBS. Antigenic heat retrieval was performed using citric acid buffer solution. A 2L beaker was taken containing 450 mL of freshly prepared citric acid buffer solution adjusted to a PH of 6. Temperature of the solution was adjusted to 68 ^{0}C. Slides were placed in this solution for 15 minutes. Following that, the entire apparatus was cooled down on bench for 15 minutes. Slides were then immersed in PBS briefly. Pretreatment with 2N hydrochloric acid at 37^{0}C was then performed for 15-20 minutes in a coplin jar. The slides were placed in the coplin jar and were washed in PBS twice for 10 minutes each on a rotating platform. After permeabilization, specimens were blocked in 0.1M Trish Ph7.5, 0.15M NaCl with PE (Perkin-Elmer FP1020) was done for at least one hour. The sections were then incubated in 1:100 dilutions of anti-BrdU antibody (ab6326, Abcam) diluted with the same blocking agent overnight (250 µl of solution per slide). Following primary antibody, samples were washed using 0.1% Triton in PBS twice for 10 minutes each. Secondary antibody was then used. The secondary antibody that was used to visualize the immunoproduct was Alexa Flour 546 Goat anti- rat IgG (Thermo Fisher Scientific)

diluted 1 to 300 in block and incubated for 60 minutes. Following the secondary antibody, samples were washed with 0.1% Triton in PBS twice for 15 minutes each and counter stained with DAPI 1: 1000 dilutions in PBS. The samples were dried moderately using Kim wipe and cover slipped using 40 μl of Prolong Gold. The percentage of BrdU positive cells to total mesenchymal cells in a fixed area was counted in the anterior and mid regions of palate shelves at E12.5. For the analysis of bend region, the total number of BrdU positive cells was also counted in a fixed rectangular area. Three samples and six palates were examined in each group and stage. The percent BrdU positive cells in the palatal mesenchyme of middle palate region and the BrdU positive cells per fixed box of the anterior palatal bend region were noted in the controls and the *Rdh10* conditional mutants and a student's t-test with unequal variance (two tailed) was performed to assess any significant differences between the control and the *Rdh10* conditional mutants.

2.8 Tongue Measurements:

The E14.5 embryonic heads (n=3) for each genotype were fixed in 4% PFA, embedded in paraffin and were sectioned in the coronal plane at 8 μm thickness. Control littermates and *Rdh10* conditional mutants were processed in parallel and used for comparison. Identical sections in the mid regions of the palate were compared between the control and the mutant taken at the same magnification using the Axiocam MRC5 microscope. Images were collected from the controls and the mutants and measurements were done using Image J. Prior to measuring, we standardized the scale to mm. A line was drawn at the base of the tongue from

one sulcus to another. A perpendicular line was then drawn from the tip of the tongue to the line previously drawn. This perpendicular representing the height of tongue was measured and noted down. Statistical analysis was performed using Excel and a paired t test was performed. Statistical significance was determined at 90% confidence interval.

2.9 Roller Bottle Culture for Maxillary Explants:

Freshly dissected maxillary explants of E13.5 embryos were cultured as described previously by Lan et al(Lan, Zhang et al. 2016).

We performed two different sets of culture experiment. During our initial analysis, three to four maxillary explants were placed in each scintillation vial containing 6ml BGJb medium (Invitrogen) supplemented with 2.8 mg/ml glutamine, 6mg/ml BSA and 1% Penicillin and Streptomycin. The bottle was flushed two minutes each day with a gas mixture (50% O_2, 45% N_2 and 5% CO_2), sealed airtight using a silicone plug and incubated at 37°C on a Wheaton Mini Bench-Top roller bottle system at a speed of 25 rpm for three days. A small piece of tissue was taken from each explant after 3 days for genotyping and explants were fixed individually. For imaging the palate shelves, these explants were then transferred to 1: 1000 dilution of DAPI in PBS and imaged using Leica M165FC Microscope. As we cultured 4 to 5 maxillae in the same scintillation vial without knowing the genotyping, we called this a combo culture.

In single/ monoculture experiment, we identified the mutants based on salivary gland or lung phenotype and cultured them together. During times when we were

unable to identify mutants and controls prior to culturing, we cultured single maxilla individual vials and the bottles were numbered. We number the tail samples from the embryo in the same way sent them genotyping. We followed the same culture technique that was followed for the combo culture. Chi Square test was performed to analyze statistical significance.

2.10 Statistical Analysis

All results were presented as mean ± SEM. All statistical analyses were done using Excel software. Two-tailed Student's t tests were used for comparisons between two groups. P value less than 0.05 was considered significant. For tongue measurements, P value of less than 0.1 was considered significant.

CHAPTER 3: RESULTS

<u>3.1 Generation of conditional *Rdh10* mutant embryos and heterozygous controls</u>

In order to generate conditional mutants, we paired *Rdh10* $^{flox/flox}$ Ert2Cre2$^{+/+}$ with

the *Rdh10* $^{-/+}$. The inducible cre-lox system was used to provide timed excision of

the *Rdh10* gene. The mutants obtained by the genetic cross (Fig. 4) are the

Rdh10 $^{flox/-}$Ert2 Cre and the controls are the heterozygous *Rdh10* $^{flox/+}$ Ert2Cre.

This means that the mutants have a normal *Rdh10* gene expression until activation

of the Cre recombinase. This activation of cre enzyme is achieved by the

administration of tamoxifen. Upon tamoxifen administration, the Cre that is bound

to the ER receptor in the cytoplasm is released into the nucleus. This causes the

excision of the exon 2 segment of the *Rdh10* gene flanked by the LoxP sites.

The excision causes inactivation of the *Rdh10* gene (Fig 5).

This genetic cross is highly useful as we obtain both the heterozygous control

embryos and the *Rdh10* conditional mutant embryos from the same litter. Based

on our genetic cross, we expect 50% of the embryos from each liter to be controls

and 50% to be mutants. This genetic cross reduces the variability and prevent bias

of the experimental set up. For example with this study design we ensure that

control embryos and the mutant embryos receive the same dose of tamoxifen, at

the same time, and are collected at the same developmental stage. This can only

be achieved when both genotypes can be produced in a single litter.

In conclusion, we were successful in creating *Rdh10* conditional mutants and these mutants were used to examine if loss of RDH10 caused cleft palate.

Genetic cross to conditional *Rdh10* mutation

Parent 1

$Rdh10^{flox/flox}(ER^{T2}Cre)$

Parent 2

$Rdh10^{-/+}$

Embryos

$Rdh10^{Conditional/-}$ Mutants

$Rdh10^{conditional/+}$ Wild type
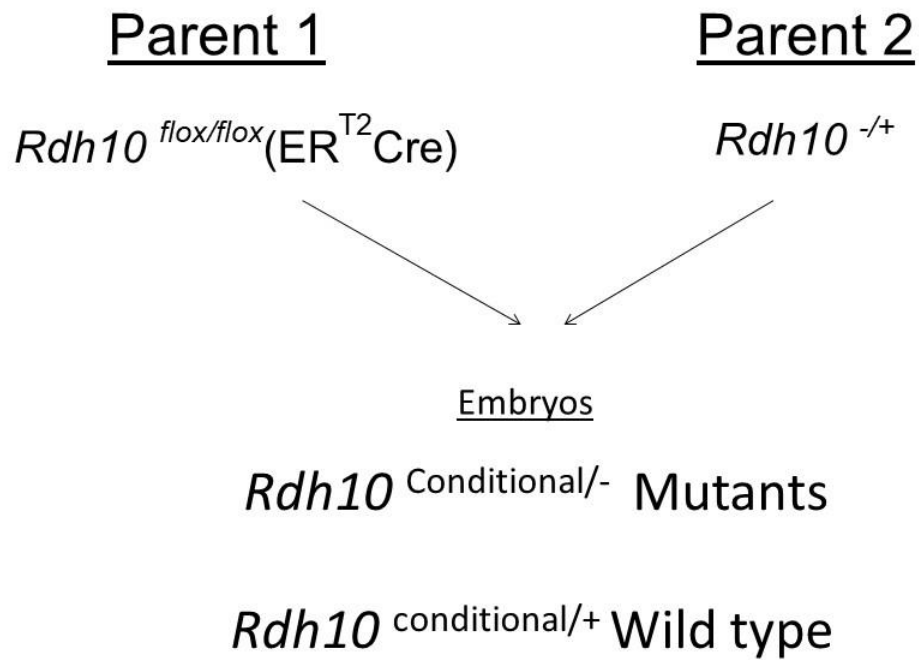
Figure 4. Generation of *Rdh10* Conditional Mutants Embryos
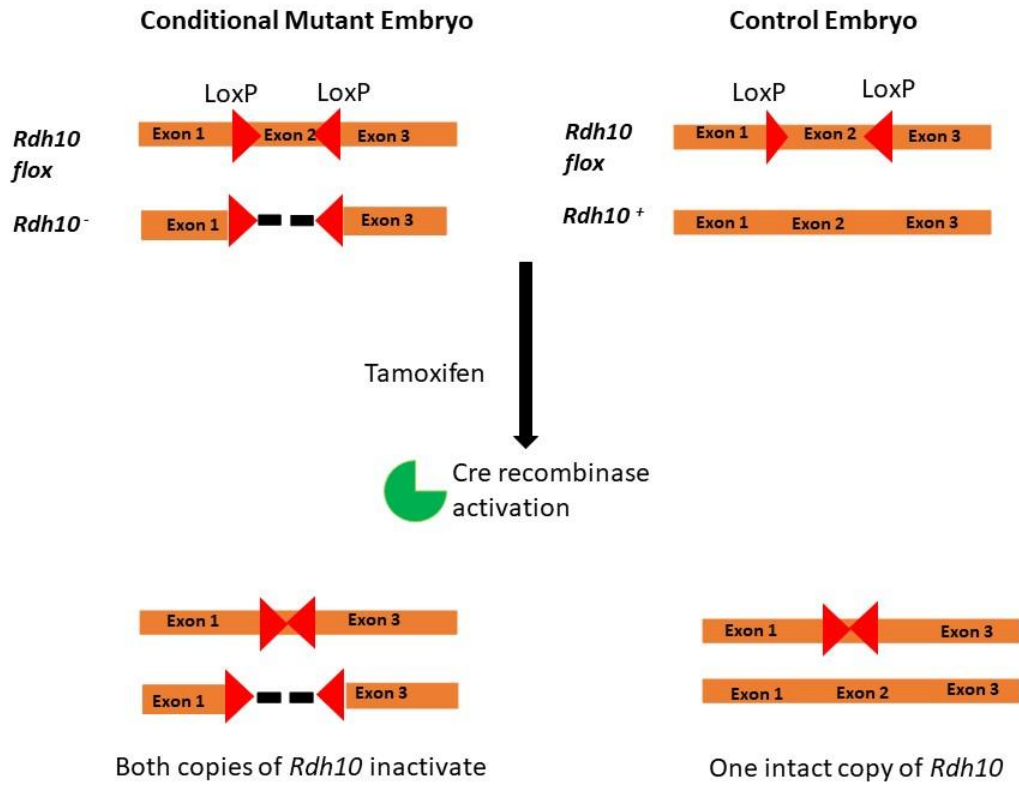
Figure 5. Inducible Cre-Lox system and generation of conditional mutants and controls.

3.2 Conditional Inactivation *of Rdh10* causes Cleft palate

In order to determine if conditional inactivation of *Rdh10* causes cleft palate, we performed a stage specific excision of *Rdh10* by tamoxifen induced conditional inactivation.

Even though we know tamoxifen, induced conditional inactivation of *Rdh10* can be performed, we did not know the optimal timing to administer tamoxifen and how long it takes to excise *Rdh10*. Therefore, we administered a single dose of tamoxifen to pregnant female mice at four different stages prior to palate formation and assessed the impact on palate formation in embryos. Tamoxifen was administered either at gestational age at E7.5, or E8.5, or E9.5 or E10.5 and harvested embryos at E16.5 to assess palate formation.

Following euthanasia of the tamoxifen-treated pregnant female mouse, embryos were isolated, decapitated and fixed in 4% paraformaldehyde. After fixation, the mandibles were removed from the embryonic heads allowing us to visualize the palate. Using nuclear florescent imaging technique, we captured and analyzed images of the palate shelves in control and mutant embryos. 100% of the control embryos showed normal palate morphology upon administration of tamoxifen at either E7.5, E8.5, E 9.5, or E10.5 (Fig. 6A). Interestingly, the *Rdh10* conditional mutants showed cleft palate at different stages of tamoxifen administration (Fig 6 B-E).

When tamoxifen was administered at E7.5, 9% of the mutant embryos showed complete cleft palate (Fig. 6B, Fig. 7). In addition to complete clefts of the

secondary palate, we also observed 19% of the mutants with minor palate abnormalities such as unilateral/ bilateral posterior truncation and incomplete cleft of the secondary palate (Fig. 6D, Fig. 7). In addition to the defects mentioned above, when tamoxifen was administered at E7.5 we also observed fewer mutants than heterozygous controls, indicating that inactivation of *Rdh10* caused embryonic lethality. We estimate that loss of *Rdh10* by tamoxifen administration at E7.5 resulted in lethality of 24% of mutant embryos prior to E16.5 (table 3). This is likely due to the fact that RA produced by RDH10 activity is not only important for the development of the palate, but also for the development of vital organs such as the heart. Due to this reason, early knockout of *Rdh10* may have caused embryonic death.

In contrast, when we administered tamoxifen at E8.5, we observed a higher percentage of palate abnormalities (58%) and we did not see any mutant lethality (Fig. 7, table 3).Following administration of tamoxifen at E8.5, mutants were obtained at the expected frequency of 50%, indicating that there was no embryo lethality at this stage. Of the mutant embryos 44% showed complete cleft of the secondary palate and an additional 14% showed minor palate abnormalities (Fig. 6E, Fig. 7, table 3).

The frequency of palate abnormalities was reduced when tamoxifen was administered at later stages. When tamoxifen was administered at E9.5, we observed 21% of the mutants with complete cleft of the secondary palate (Fig. 7, table 3). The percentage of minor palate abnormalities was 32%. The frequency of minor palate abnormalities was higher at the E9.5 tamoxifen stage compared to

other stages of tamoxifen administration. No mutant lethality was noted at this stage.

No palate abnormalities were observed in the mutants when tamoxifen was administered at E10.5 (table 3). We did observe some embryo lethality at this stage. However, the percentage embryo lethality and phenotype may not be significant owing to the small sample size analyzed.

From the above results, we can conclude that the highest percentage of cleft palate with minimal mutant lethality was observed upon administration of tamoxifen at E8.5. Hence, further experiments to understand the mechanistic role of *Rdh10* deficiency in the development of cleft palate was done by administering tamoxifen at E8.5.

In summary, loss of *Rdh10* causes cleft palate. When 100% of the controls show normal palate phenotype at E16.5, 44% of the mutants show complete cleft palate when tamoxifen is administered at E8.5. Therefore, we show that conditional inactivation model serves to be an effective way to understand how RA deficiency affects palate development

In addition to establishing a model system that will allow us to improve our knowledge on how RA deficiency affects palate development, the results obtained from this experiment also hints at the time frame when RA maybe needed during palate development. Early administration of tamoxifen at E7.5 caused mutant lethality while later stages of administration (E9.5 and E10.5) showed reduced frequency of cleft phenotype, suggesting that *Rdh10* mediated metabolism of RA

may be needed during specific time frame at early stages of palate development. This finding directed our next set of experiments towards understanding the role of RA in early palate morphogenesis.

Control

Rdh10 Conditional Mutants
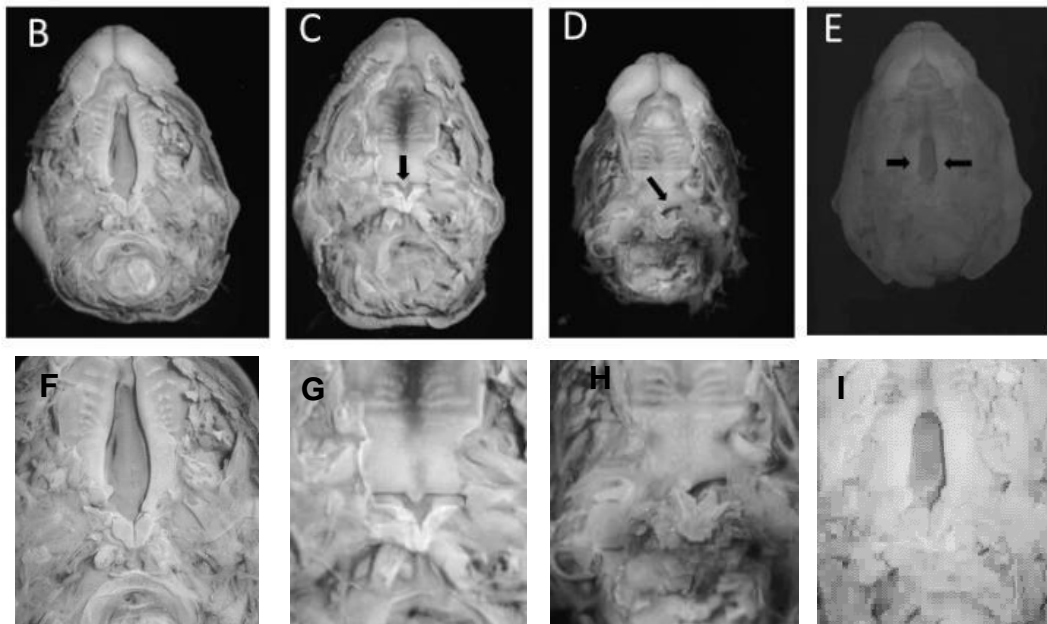
Figure 6. Morphological analysis of *Rdh10* mutant maxilla. Nuclear florescent imaging of E16.5 control(A) and mutants (B-E). (B) showing complete cleft of the secondary palate in mutant. (C), (D), & (E) showing minor palate abnormalities. Arrow in (C) shows a bilateral posterior truncation seen in the soft palate. Arrow in (D) shows a unilateral posterior truncation seen in the soft palate. Arrows in (E) show an incomplete posterior cleft extending into the hard and the soft palate.(F-I) showing a closer version of the defects (B-E)

Mutant phenotype following conditional Rdh10 mutation
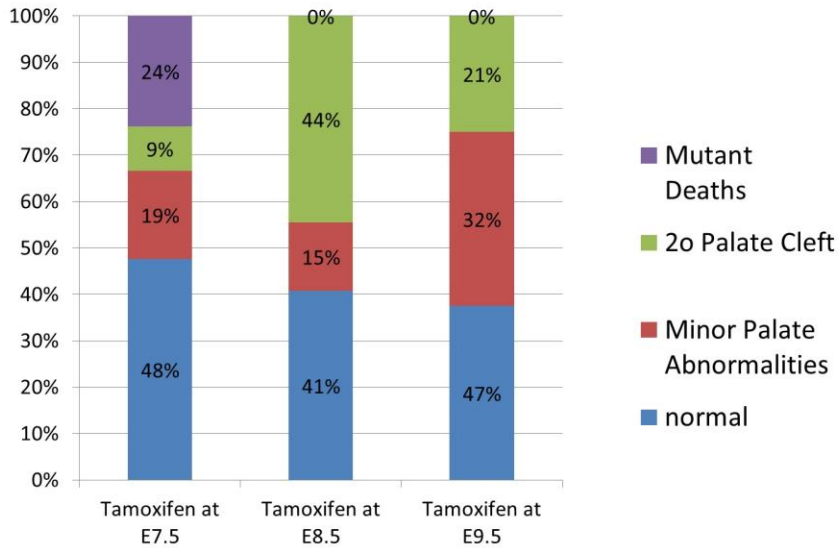
Figure 7. Percent cleft palate distribution and embryo viability at different stages of tamoxifen administration. 24% of mutant lethality is seen when tamoxifen was administered at E7.5. Tamoxifen administered at stage E8.5 showed maximum percentage of cleft – 59% of the mutants examined at E8.5 showed some defects in secondary palate formation. Of the 59% 44% of the mutants showed complete secondary palate cleft and 15% showed minor palate abnormalities. As we administered tamoxifen later during embryonic development (T9.5, T10.5), we see a fewer percentage of cleft to almost no palate abnormalities when tamoxifen is administered at E10.5. This gradual reduction in phenotype with progression in stage of administration likely suggest an early role of *Rdh10* mediated RA during palate morphogenesis.

	Total Number of embryos examined	Number of Hets	Number of Hets (Expected)	Number of Mutants	Number of mutants (Expected)
E16.5 T7.5	42	26	21	16	21
E16.5 T8.5	48	21	24	27	24
E16.5 T9.5	37	18	19	19	19
E16.5 T10.5	17	11	8	6	8

Table 3. Distribution of embryo genotype that we expected and obtained at different stages of tamoxifen administration. We note that the total number of mutants that was expected at E7.5 is more than the mutants obtained. According to our genetic cross, we need to get 50% of heterozygous controls and mutants per litter. However, since the number of mutants obtained was less than the expected, early administration of tamoxifen at E7.5 might have caused some mutant lethality. Even though the number of mutants observed at E10.5 is also less, this may be due to fewer litters observed at this stage.

3.3 RA Signaling in the Palate at E12.5:

Previous studies of RA activity in developing facial tissues have not identified active signaling within the palate. From result 3.2, it is clear that RA is needed for palate development. In other words, loss of RDH10-mediated RA production leads to cleft palate. In order for us to understand the possible mechanistic role of RA during the development of palate, we wanted to see if there is any detectable RA signaling within the developing palate shelves. The RARE-Lac Z reporter mouse was used to understand the spatiotemporal distribution of RA within the palate shelves. The RARE-LacZ reporter mouse line was generated by Rossant et al (Add reference!),in which bacterial LacZ gene was placed under the RA receptor element. Detection of the reporter gene expression is identified dark blue X-gal stainwhich indicates cells that have active RA signaling. In order to examine if RA signaling activity was present in developing palate shelves we harvested RARE-LacZ embryos at E12.5 when early palate shelf growth occurs. We exposed the palate by removing the mandible and tongue and performed X-gal staining. This helped us capture even the weakest RA signaling within the palate shelves.

The whole mount images of the LacZ stained embryos revealed strong RA signaling in the developing nasal sinus region and the primary palate. Careful examination of the secondary palate revealed a small patch of signaling in the anterior-most region of the developing palate shelves (Fig. 8). The precise tissue distribution of the RA signaling was analyzed by paraffin sectioning of the whole-mount stained heads. Frontal sections were then counter-stained with Nuclear Fast Red.

Consistent with previous studies, no RA signaling activity was detected in the posterior or middle palate shelf tissue (Fig 9 A, B). However, careful histological analysis reveals for the first time that RA signaling is present in the developing secondary palate at E12.5. RA signaling was seen in the epithelium of the bend region of the anterior palate shelf and the sub-nares anterior zone (SNAZ) (Fig 9 C-F). Although RA signaling was detected in the epithelium of the SNAZ and bend region, no signaling was detected in the middle palate and the posterior palate regions. We also did not detect any signaling in the mesenchyme of the palate shelf at any regions at E12.5.

This finding is extremely valuable in our field of study. Not only has there been a gap in knowledge regarding the role of RA in palate development, but also no reported finding of RA signaling within the palate shelf tissues (Okano, Kimura et al. 2012).

Collectively, these data suggest that RA signaling is seen in the developing palate shelf at an appropriate time to play an important role in its development. This RA signaling may be an important intrinsic factor essential for normal development of the secondary palate.
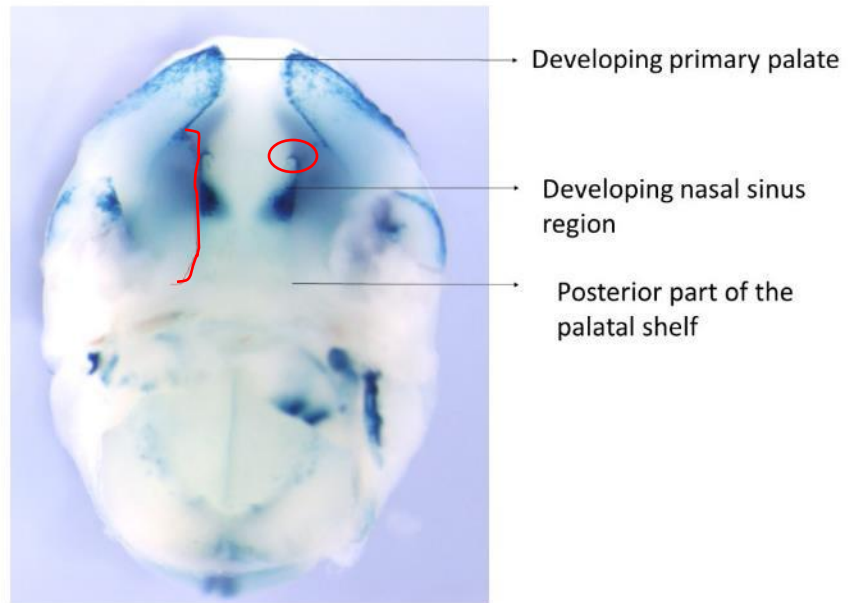
Figure 8. Activity of RARE LacZ in developing secondary palate. Whole Mount ß galactosidase staining of developing palate at E12.5 with the tongue and mandible removed. Dark Blue areas reveal RAR activity (A). We can see strong signaling in the developing primary palate and the nasal sinus region. The red line depicts the palate shelf outline on the left side. Since signaling in sinus is very strong, it is difficult to identify signaling in the anterior region of the palate shelf depicted by the red circle without sectioning.
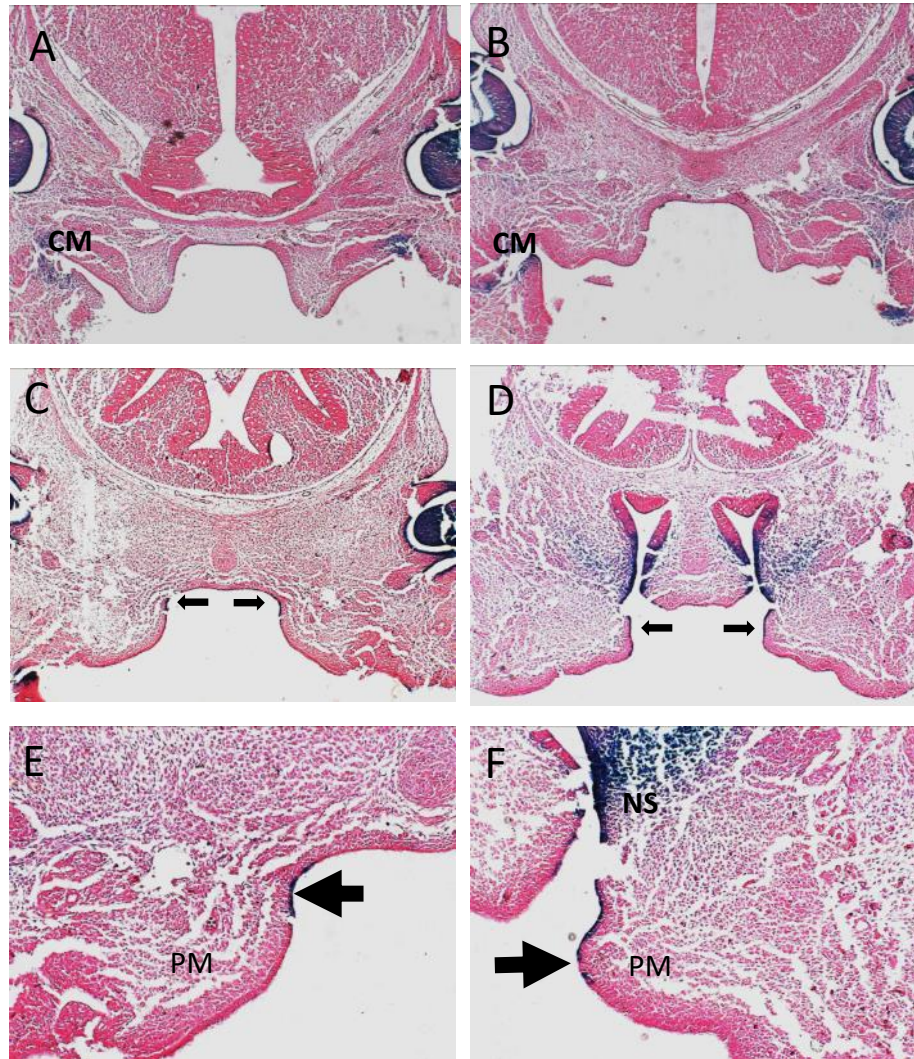
Figure 9. Histological sections stained with nuclear fast red showing RARE LacZ activity. Frontal sections showing the posterior part of the palatal shelf (A), middle part of the palatal shelf(B), anterior part of the palatal shelf(C) and the sub nares anterior zone(SNAZ) (D) of the developing secondary palate at E12.5 taken at 4X magnification. Although some RA signaling activity is seen the corner of the mouth in the posterior region and the middle region of the palatal shelves at E12.5, no detectable signaling seen in the palatal shelf epithelium or mesenchyme in these regions (A&B). E&F are the same sections as C&D taken at 10X magnification.10X view of the anterior region showing RA activity in the bend region of the palate (E).10X view of the SNAZ region of the developing secondary palate showing RA signaling activity within the epithelium of the palate shelf. (F). Arrow indicates RA signaling in the epithelium of developing palate shelf tissues. No signaling detected in the mesenchyme at this stage. CM- corner of the mouth; NS- Nasal Sinus; PM- Palatal mesenchyme.

<u>3.4 *Rdh10* conditional mutants not only display intrinsic defects in early palate morphogenesis, but also extrinsic defects in tongue positioning.</u>

Now that we have a model system that allows us to study the role of endogenous RA, we can try to understand the underlying mechanisms it regulates in the palate. Palate development, as described above (Fig. 2), is a sequential process that occurs beginning early E11.5 up to E16.5. Since we see cleft palate in *Rdh10* conditional mutant embryos at E16.5 by whole mount imaging (Fig. 6 B-E), we examine the palate tissues of control and mutant embryos by histological staining at E16.5.

Histological sections taken at E16.5 of the heterozygous controls and the *Rdh10* conditional mutants is shown in Fig 10 A-D. Inadequate growth and improper elevation of palate shelf tissue along with abnormal positioning of the tongue are some of the findings in the mutants compared to the controls. Growth and elevation of palate shelf tissues are early events that occur during secondary palate development. The defects seen at E16.5 are defects that must have occurred during early stages of palate development. These early defects along with early RA signaling seen at E12.5 (Result 3.2) once again suggest an early role of RA during palate development. All our previous results have suggested a possible role of RA in early palate morphogenesis. Therefore, in order to understand the mechanism of palate defects resulting from loss of *Rdh10*, we examined embryos at different early stages of palatogenesis *i.e.* E12.5, E13.5 and E14.5 after administration of tamoxifen at gestational stage E8.5.

Morphological variations observed using hematoxylin and eosin (H&E) staining revealed abnormalities in the palate shelf tissue of mutant embryos as early as E12.5. We compared three controls and three mutants at this stage. H& E staining of the anterior, middle and the posterior region of the palatal shelves revealed shorter palatal shelves in the mutants compared to the control (Fig. 11 A-F). All the mutants observed at this stage showed lack of groove between the palate shelf tissue and the body of the maxilla in the mid sections of the developing secondary palate (Fig. 11 D). Moreover, the palatal shelf outgrowth in the anterior region was reduced in the mutants compared to the control (Fig. 11 F).

Morphological abnormalities were also observed in mutant embryos at E13.5. Mutant embryos examined at E13.5 revealed a sharp bend region (Fig 12) compared to the more rounded bend morphology of the controls. We examined three controls and three mutants at this stage and all three mutants revealed this phenotype.

We also harvested and sectioned embryos at E14.5. Variations in palate shelf orientation was observed at this stage in both the controls and the mutants. Of the six controls sectioned, three controls showed palate shelves that had elevated and contacted in midline, and three showed vertically oriented palate shelves. Of the six mutants sectioned, two mutants showed horizontally oriented palate shelves contacting in midline, one showed asymmetric elevation of palate shelf and 3 showed vertical orientation of palate shelves.

We wanted to compare the tongue height in *Rdh10* conditional mutants and the controls that had a vertically oriented palate shelf at E14.5. We looked at the mid palate sections from three controls and three mutants. We found that *Rdh10* conditional mutants showed taller tongue compared to controls (Fig 13 and table 4). Statistical significance was obtained at $p<0.1$.

In addition to the taller tongue at E14.5, we also noted abnormal fusion between the mandible and the palatal shelf in two of the three mutants examined. Abnormal shelf-to-mandible contact and loss of epithelium in the developing mandible and palate was noted with mesenchymal cell fusion (Fig.14). Abnormal shelf-to-mandible contact may cause cleft palate by preventing the elevation of palate shelves. However, our mutants that showed such fusion in the posterior region of the developing palate shelves showed palatal shelves contacting at the midline in the anterior and middle region. This observation suggest that, abnormal shelf-mandible fusion may result in minor palate abnormalities and not be directly involved in causing cleft palate in *Rdh10* conditional mutants.

In summary, defects in early palate morphogenesis are detected in *Rdh10* conditional mutant embryos. Abnormalities in palate morphology can be seen as early as E12.5. *Rdh10* mutants show sharp bend regions at E12.5 and taller tongues and shelf-to-mandible fusion at E14.5. The presence of RA signaling within palate shelf tissues (Fig. 9) and the defects in early palate shelf morphology suggest that the loss of *Rdh10* could cause cleft palate by a mechanism intrinsic to the palate shelf tissues. However, we cannot eliminate the fact that we also see taller tongues and shelf-to-palate fusion in *Rdh10* mutants. Taller tongues could

cause cleft palate by a mechanism extrinsic to the palate shelf tissues if the abnormal positioning of the tongue interferes with the elevation of palate shelves.
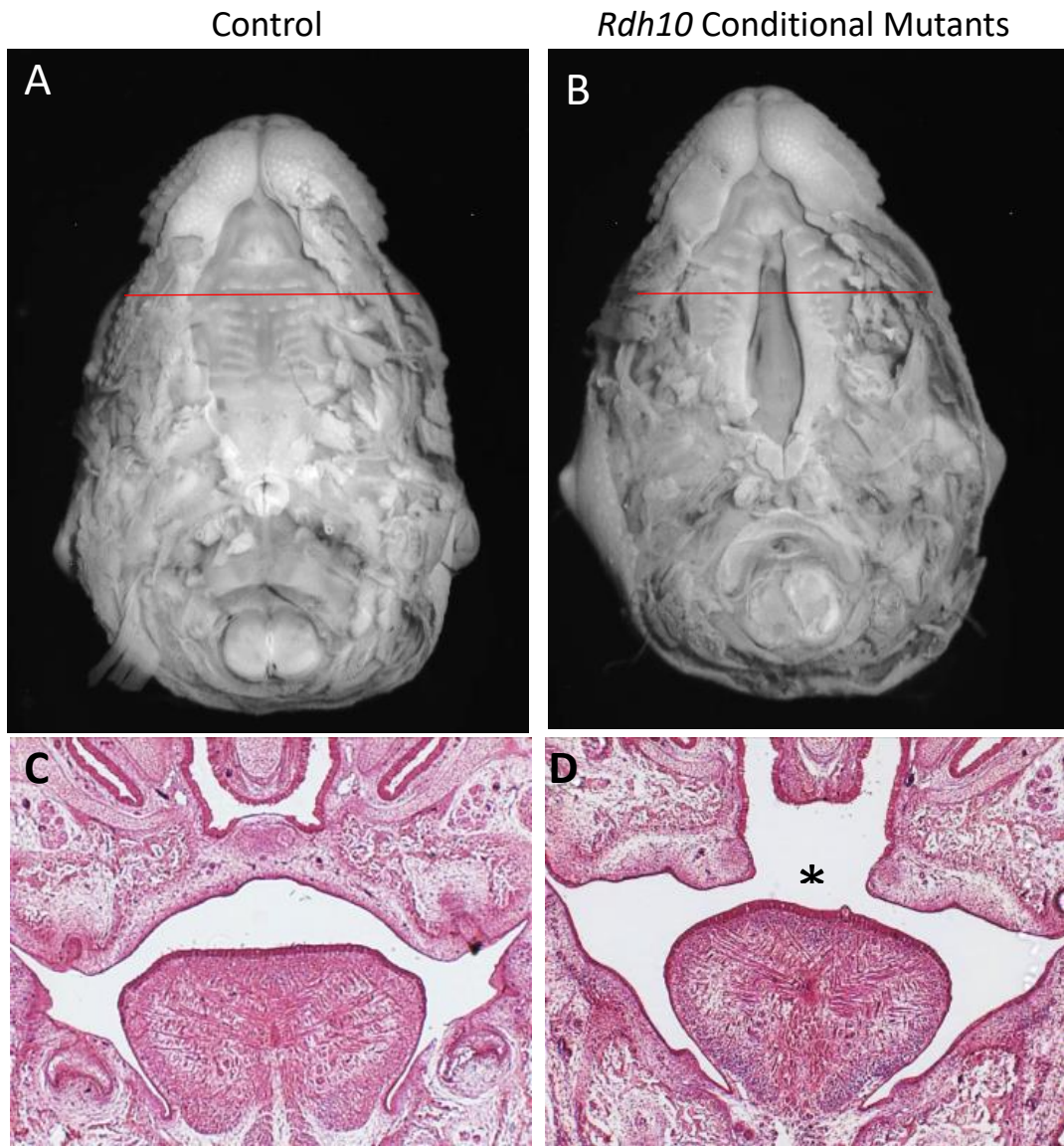
Figure 10. Morphological and histological comparison of control and *Rdh10* conditional mutant at E16.5. Nuclear florescent image of palate of control (A) and *Rdh10* conditional mutants. (B)The red line on DAPI images (A&B) showing the location of palate of H&E stained coronal sections from the control (C) and the *Rdh10* conditional mutants(D) at embryonic age E16.5 (D) showing inadequate growth and improper elevation of palate shelves. Abnormal tongue musculature also seen in the mutants compared to control littermates.

A Control
B *Rdh10* Conditional Mutants

Posterior

C
D

Middle

MAX PS

E
F

Anterior
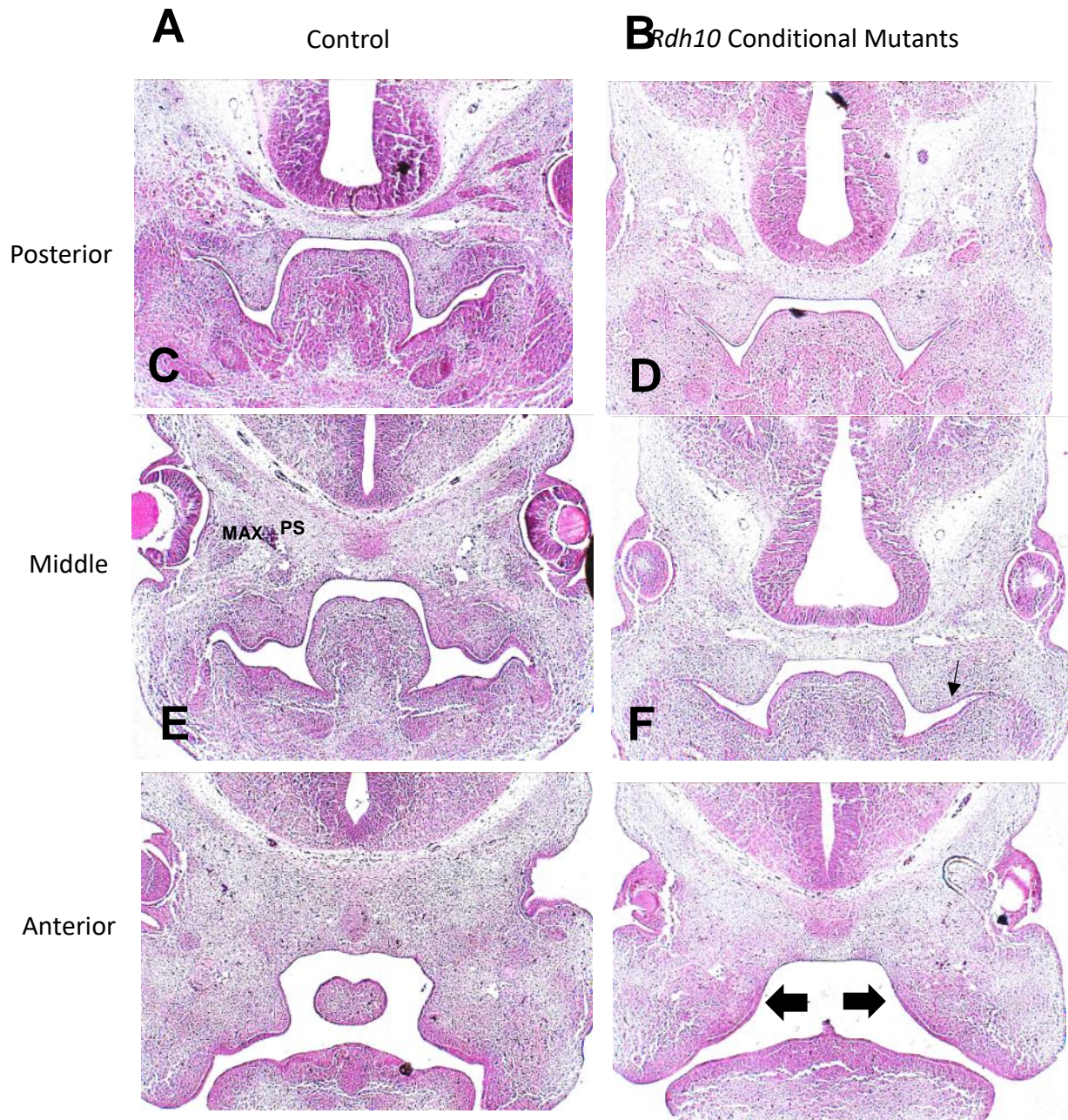
Figure 11. *Rdh10* conditional mutants showed morphological defects in palate shelves as early as E12.5. Hematoxylin and Eosin stained coronal sections of E12.5 control and *Rdh10* conditional mutant embryos. (A-F). Shorter palate shelves in posterior region seen in Rdh10 conditional mutants (B) compared to control littermates (A). Lack of mid palate groove between the palate shelf and body of maxilla also seen in mutants (D) compared to control(C) in the mid palate region. Reduced palate shelf outgrowth seen in the *Rdh10* conditional mutants (F) compared to controls in the anterior region of palate shelves. Arrow indicates region of defect.PS- Palatal shelf; Max- Body of Maxilla

46
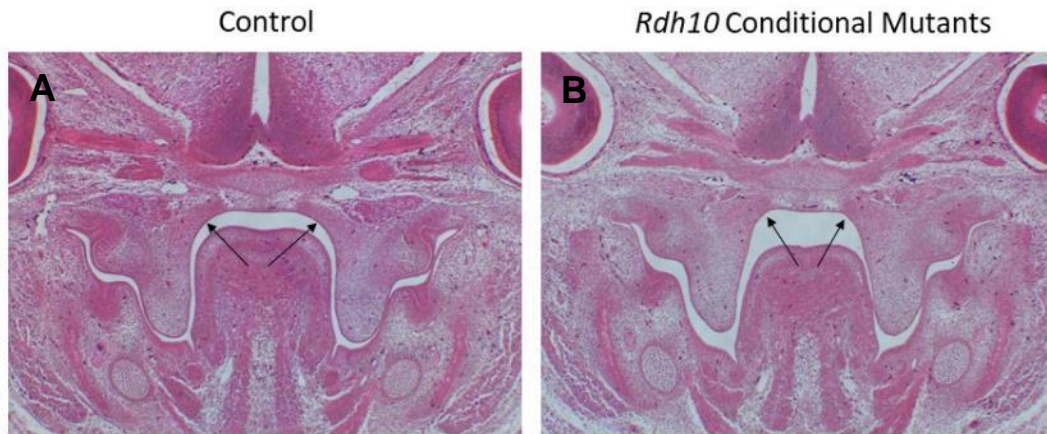
Figure 12. *Rdh10* conditional mutants display a sharp bend region at E13.5. Coronal sections of E13.5 showing the posterior palate shelves in the control (A) and *Rdh10* Conditional mutants (B) Arrows indicate the bend region. Three of the three mutants examined showed this abnormality compared to the control embryos.
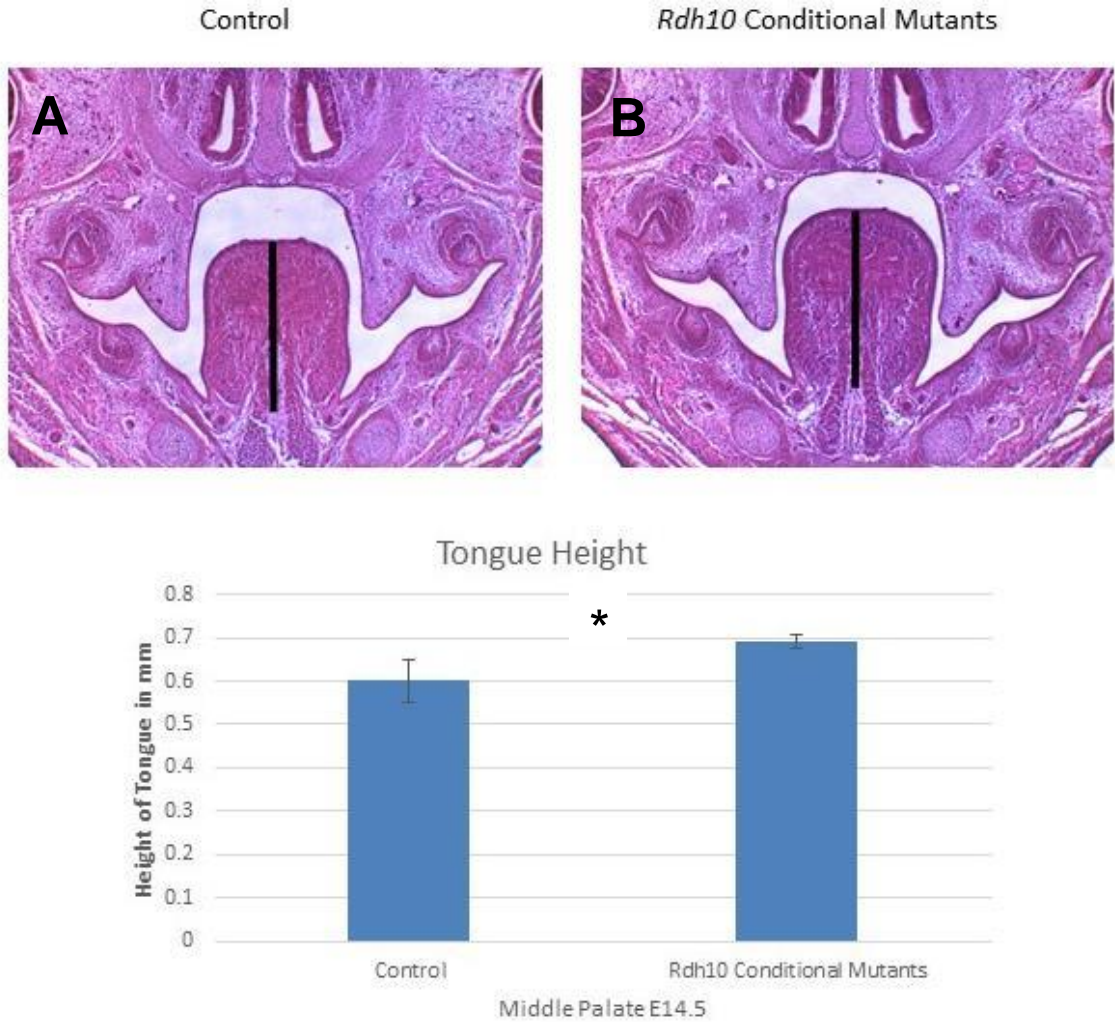
Figure 13. *Rdh10* conditional mutants show taller tongue. (A) Shows heterozygous control and (B) represents *Rdh10* conditional mutant. Measurement of tongue height were compared as demonstrated by the black line in A & B (n=3). Statistical significance is denoted by the * over the bar graph. (P<0.1)

Height of Tongue(in mm)

Control 1	0.608
Control 2	0.647
Control 3	0.55
Avg	0.601667
Mutant 1	0.703
Mutant 2	0.672
Mutant 3	0.697
Avg	0.690667

t-Test: Two-Sample Assuming Unequal Variances

	Controls	*Mutants*
Mean	0.601667	0.690667
Variance	0.002382	0.00027
Observations	3	3
Hypothesized Mean Difference	0	
df	2	
t Stat	-2.99302	
P(T<=t) one-tail	0.047925	
t Critical one-tail	2.919986	
P(T<=t) two-tail	0.09585	
t Critical two-tail	4.302653	

Table 4. T test table for height of tongue. The first table representing raw data obtained. Measurements shown are in mm and was obtained using Image J. t test assuming unequal variance was obtained using Microsoft excel. Statistically significant data was obtained at $p < 0.1$ level.

Control   *Rdh10* Conditional Mutants
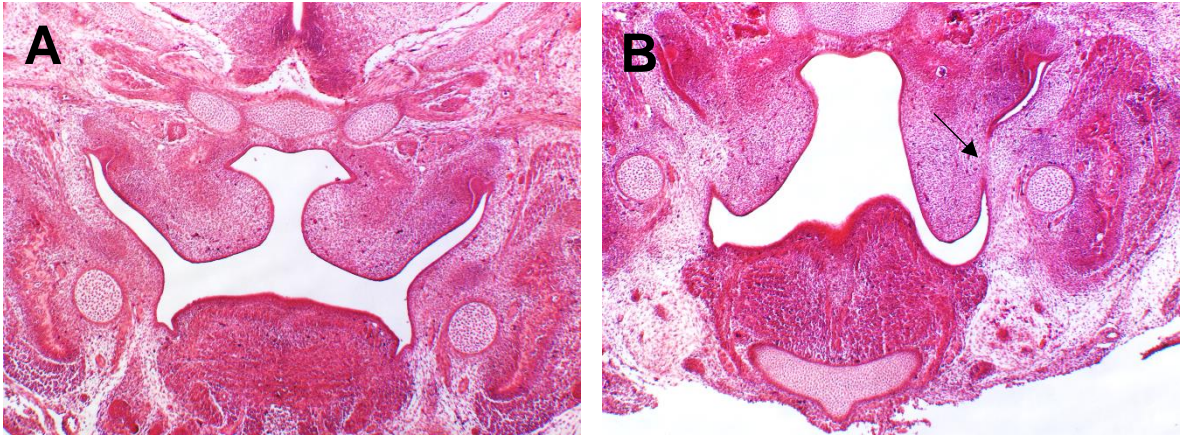
Figure 14.*Rdh10* conditional mutations show palate-oral fusion compared to controls at E14.5. Coronal H& E sections through E14.5 control (A) and *Rdh10* Conditional mutant (B) littermates in the posterior palate shelf region. Arrow indicates the position of the abnormal fusion in mutant.

3.5 Increased Defects in Proliferation of Palatal Mesenchyme seen at E12.5:

To investigate the intrinsic role of RA in cleft palate, we examined cell turn-over by BrdU incorporation. We chose to study cell proliferation over other cellular mechanisms that could be altered because excess RA has been shown to have an effect on cell proliferation in the palate (Okano, Kimura et al. 2012). We wanted to see if our *Rdh10* conditional mutants showed altered cell proliferation. Because we observe RARE-LacZ activity within the developing palate at E12.5, we assessed the regulation of cell proliferation in the mesenchyme of palate shelves at that stage. Since a clear morphological difference was seen in the anterior and mid palate regions in the mutants compared to controls, we decided to measure proliferation in these regions. We therefore administered BrdU to tamoxifen-treated pregnant mice at E12.5. Embryos were harvested 3 hours after BrdU exposure, fixed, sectioned, and immunostained for presence of BrdU incorporated into DNA.

 In order to quantify the percentage of cells within the palate shelves that had incorporated BrdU into their DNA, fter immunostaining and imaging, we marked the outline of palate shelf outgrowth in both the controls and the mutants using the ImageJ software. We then counted the total number of DAPI positive nuclei in the mesenchyme and the epithelium of the palate shelf and the total number of BrdU positive cells per palate shelf (Table 5 & 6). The ratio of BrdU positive cells to the total number of DAPI positive cells was compared between the heterozygous controls and the *Rdh10* conditional mutants in anterior and mid coronal sections (Fig 15). Even though the palate shelf outgrowth happened to be smaller in the

conditional mutants with reduced total number of cells, no statistical difference was noted in percent of BrdU positive cells in the mesenchyme of the palate shelves.

We also wanted to see if there was any difference in proliferation at the bend region where RA signaling is seen. We therefore outlined a fixed-size box in the bend region of control and mutant embryo images and counted the total number of BrdU positive cells per fixed box. The proliferation in the proximal bend region of the palate shelf was significantly increased in the *Rdh10* conditional mutants compared to their heterozygous control littermates at $p<0.05$ significance level (Fig 16).

SNAZ Region Mesenchyme		Total number of cells	Brdu Postive Cells	Percent of Brdu Postive Cells
	Control 1R	118	51	43.220339
	Control 1L	167	65	38.9221557
	Control 2R	190	84	44.2105263
	Control 2L	187	84	44.9197861
	Control 3R	201	95	47.2636816
	Control 3L	212	105	49.5283019
			Avg=	44.6774651
	Mutant 1R	108	43	39.8148148
	Mutant 1L	110	48	43.6363636
	Mutant 2R	74	39	52.7027027
	Mutant 2L	92	36	39.1304348
	Mutant 3R	149	64	42.9530201
	Mutant 3L	103	42	40.776699
			Avg=	43.1690058

Table 5. Percentage of BrdU positive proliferating cells in the anterior mesenchyme.

Mid Palate Mesenchyme		Total number of cells	Brdu Positive Cells	Percent of Brdu Positive Cells
	Control 1R	365	93	25.4794521
	Control 1L	289	80	27.6816609
	Control 2R	282	74	26.2411348
	Control 2L	334	88	26.3473054
	Control 3R	296	102	34.4594595
	Control 3L	250	74	29.6
			Avg=	28.3015021
	Mutant 1R	192	94	48.9583333
	Mutant 1L	280	70	25
	Mutant 2R	284	88	30.9859155
	Mutant 2L	291	75	25.7731959
	Mutant 3R	197	92	46.7005076
	Mutant 3L	198	84	42.4242424
			Avg=	36.6403658

Table 6. Percentage of BrdU positive proliferating cells in the mid palate mesenchyme

t-Test: Two-Sample Assuming Unequal Variances-SNAZ Mesenchyme

	Control	Mutants
Mean	44.67747	43.16901
Variance	13.14854	24.88805
Observations	6	6
Hypothesized Mean Difference	0	
df	9	
t Stat	0.599113	
P(T<=t) one-tail	0.281936	
t Critical one-tail	1.833113	
P(T<=t) two-tail	0.563872	
t Critical two-tail	2.262157	

t-Test: Two-Sample Assuming Unequal Variances- Mid Palate Mesenchyme

	Control	Mutants
Mean	28.3015	36.64037
Variance	11.20374	114.3917
Observations	6	6
Hypothesized Mean Difference	0	
df	6	
t Stat	-1.82262	
P(T<=t) one-tail	0.059095	
t Critical one-tail	1.94318	
P(T<=t) two-tail	0.118191	
t Critical two-tail	2.446912	

Table 7. Analysis of lack of significance of percentage of BrdU-positive proliferating cells in anterior and mid-palate mesenchyme. Student t test assuming unequal variance was completed for three samples each from control and *Rdh10* conditional mutants. Observations are shown as six as it includes right and left shelf from three different samples. P values obtained is more than 0.05, allowing us to conclude that there is no difference in percent of BrdU positive cells between the control and the *Rdh10* conditional mutants in both the mid palate and SNAZ mesenchyme.

t-Test: Two-Sample Assuming Unequal Variances

Total Proliferating Cells in SNAZ mesenchyme

	Control	*Mutants*
Mean	80.66667	45.33333
Variance	389.0667	99.86667
Observations	6	6
Hypothesized Mean Difference	0	
df	7	
t Stat	3.914132	
P(T<=t) one-tail	0.002896	
t Critical one-tail	1.894579	
P(T<=t) two-tail	<mark>0.005793</mark>	
t Critical two-tail	2.364624	

t-Test: Two-Sample Assuming Unequal Variances

Total Proliferating Cells in Mid-Palate Mesenchyme

	Controls	*Mutants*
Mean	85.16667	83.83333
Variance	125.7667	91.36667
Observations	6	6
Hypothesized Mean Difference	0	
df	10	
t Stat	0.221642	
P(T<=t) one-tail	0.414527	
t Critical one-tail	1.812461	
P(T<=t) two-tail	0.<mark>829054</mark>	
t Critical two-tail	2.228139	

Table 8. Analysis of significant difference seen in the total proliferating cells in the anterior mesenchyme. No significance in proliferating cells seen in mid palate mesenchyme Student t test assuming unequal variance was completed for three samples each from control and *Rdh10* conditional mutants. Observations are shown as six as it includes right and left shelf from three different samples. P values obtained is less than 0.05, allowing us to conclude that the total proliferating cells in the palate mesenchyme at SNAZ region was fewer in mutants compared to control. However, no difference in total proliferating cells was noted in mid palate mesenchyme.
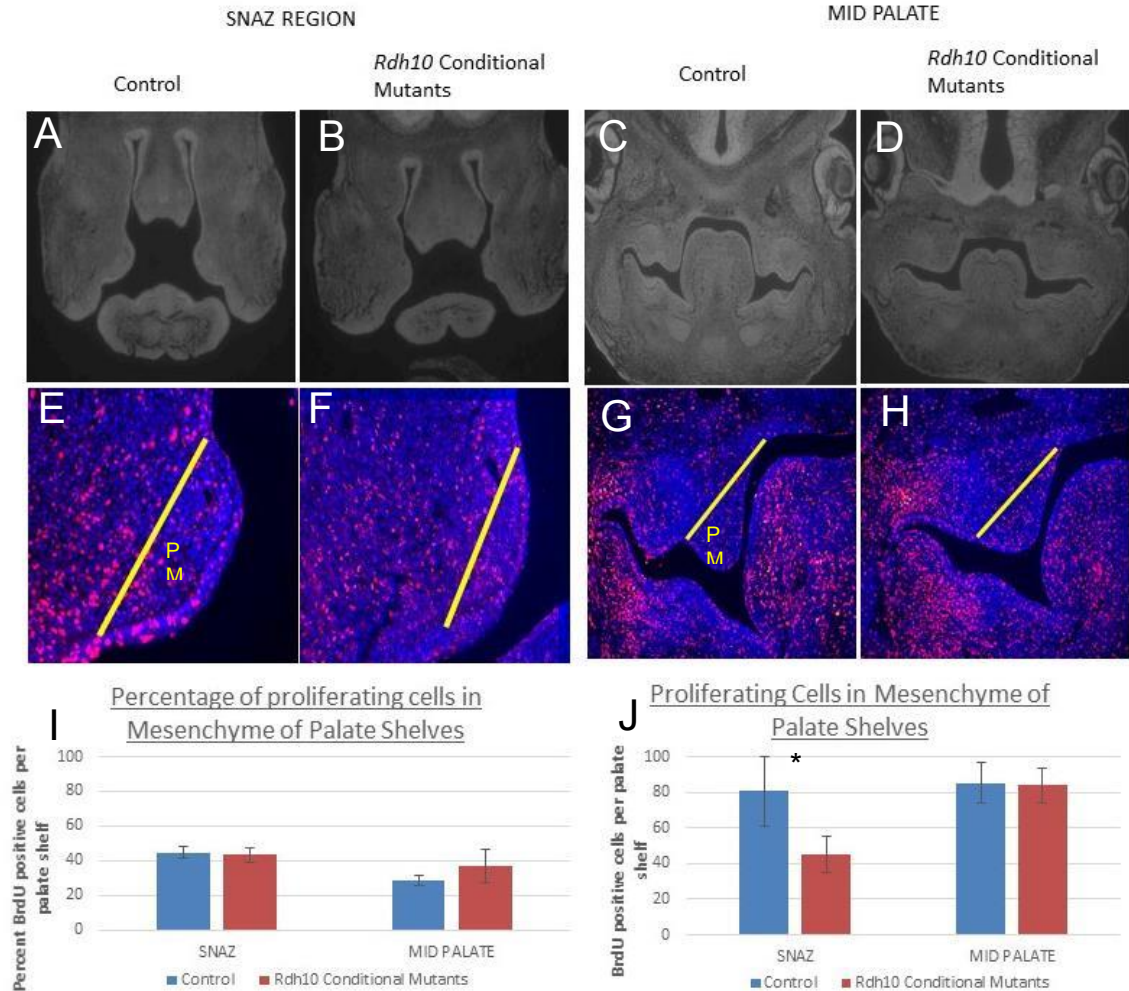
Figure 15.Comparison of proliferating cells and percent BrdU positive cells between control littermates and *Rdh10* conditional mutants in the palatal mesenchyme of the SNAZ region and mid palate region of palate shelves. DAPI images of the coronal sections from the control littermate (A) and *Rdh10* conditional mutant (B) taken in a 4X magnification that were compared in the SNAZ region. DAPI images of the coronal sections from the control littermate(C) and *Rdh10* conditional mutant (D) taken in a 4X magnification that were compared in the mid palate region. Yellow line indicates the outer border of palatal shelf up to which cell counting was made. Graphical representation of the percent BrdU positive cells in these regions in the control and *Rdh10* conditional mutants shown in fig (I) Graphical representation of the number of BrdU positive cells per palate shelf in the SNAZ and mid palate mesenchyme in these regions in the control and *Rdh10* conditional mutants shown in fig (J). Three sections from the wild type and the mutant were compared. P<0.05 was considered statistically significant. Error bard represent Stdev. * indicates significance. PM- Palatal Mesenchyme.
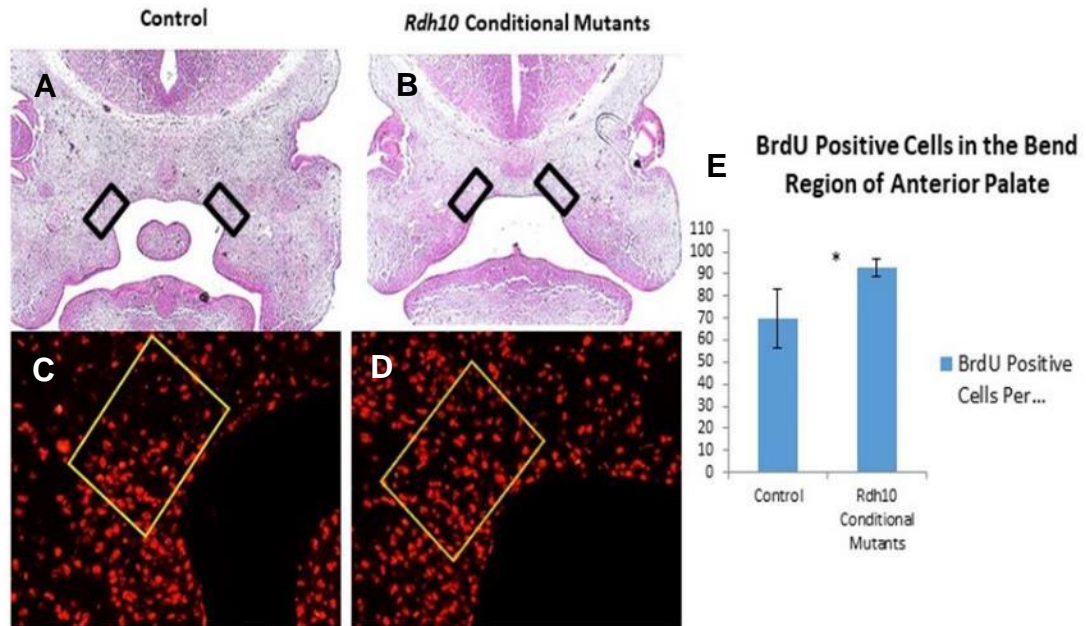
Figure 16. *Rdh10* conditional mutants show an increase in cell proliferation at the bend region in the mesenchyme of anterior palate shelf at E12.5. (A) and (B) showing 4x Hematoxylin and Eosin coronal section of the anterior region of palate shelf at E12.5. Black box indicates 4x view of image (C) and (D). (C) and (D) represents immunofluorescence staining. Red cells indicating BrdU positive cells. Proliferating cells in bend region counted per fixed box as outlined by the yellow rectangles in (C) and (D). (E) represents the graphical presentation of the values obtained. * represents statistical significance at p<0.05.

3.6 Ex-Vivo Culture of Isolated Maxilla Suggest an Extrinsic Role for RDH10 during Palate Development

Although cell proliferation assay suggests an intrinsic defect within the palate shelf with increased cell proliferation in the bend region in the mutants compared to the controls, it is possible that the failure of palate shelf elevation could be secondary to defects in abnormal tongue and mandible. To investigate this possibility, we performed a 36 hours' suspension culture of the maxilla with mandible and tongue removed.

Control and mutant embryos were harvested at E13.5 after administration of tamoxifen at E8.5. The heads were separated from the body. The maxillae were isolated from remaining part of the head by removal of the mandible, forebrain, and hindbrain. The micro dissected maxillary explants were then suspended in culture containing modified BGJb medium for 3 days as described in chapter 2. Since we did not know the genotype of the embryos, initial experiments were carried out by culturing 3 to 4 maxilla's together in each scintillation vial, and a small piece of tissue was removed after culture for genotyping purposed. We named this type of culture as a "combo" culture. The Vials were gassed with 50% O_2, 5% CO_2, and balance N_2 each day for two minutes. Genotyping was done after completion of the culture experiment. The maxillae were fixed and imaged using the pseudo SEM method described previously.

The results that we obtained from the first combo culture is depicted in Fig.17. The fusion rate of palate shelves observed in the mutants was more than that of the controls. Interestingly, we observed more fusion in the mutants grown with the

controls in the same vial. Cleft palate was seen in controls that were grown together with these mutants. No cleft palate was observed in controls that were cultured with other control maxillae in the same vial. Moreover, all mutants that were cultured together in the same vial showed cleft palate. These initial results led us to speculate that when control maxillae are cultured with mutants, it is possible that the RA produced in the controls can cross from one tissue to the other to help in the growth of palate shelves in mutants.

To test this hypothesis, we decided to perform a "monoculture" whereby maxillae of mutant embryos were cultured in vials separate from controls. Sometimes, we were able to predict the genotype of the mutant embryos based on their small salivary gland phenotype or a characteristic branching defect in mutant lungs. In such cases, 2-4 mutant maxilla were suspended together in each vial, and the controls in different vials. In other cases, we culture each individual maxilla in an independent vial. In a total of seven monoculture experiments, the incidence of cleft palate that we observed in the mutants was 22.83% and that in the controls was 12.50% (Fig 18). These data indicate that mutant palates fuse at a frequency similar to controls when cultured *ex vivo* without mandible and tongue.

In order to determine if the fused mutant cultured maxillae had evidence of sub mucous cleft or other histological defects, we processed three controls and three mutants from three different culture experiments for histological examination. On examination of the H & E stained sections, we observed that of the three-control culture maxilla, two-showed incomplete fusion with remaining midline epithelial seam and one showed complete fusion (Fig 19). Compared to controls, two of the

60

three mutants showed complete fusion and one showed incomplete fusion with remaining midline epithelial seam. Comparing these findings, we can say that no significant difference in midline fusion was seen in the *Rdh10* conditional mutants compared to the heterozygous controls after 72 hours' culture.

These results suggest that the cleft of the secondary palate seen in RA deficiency is predominantly due to an extrinsic defect in either the mandible development or abnormal positioning of tongue rather than an intrinsic role in palate itself.

Fusion Rate of Maxillary Explant Combo Culture
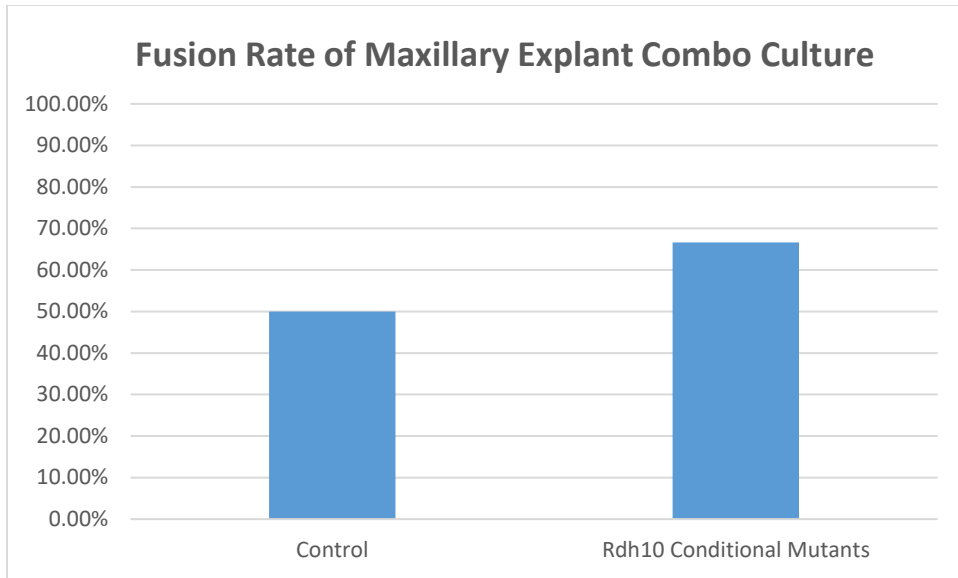
MAXILLARY EXPLANT COMBO CULTURE

	Total Maxilla Cultured	Total Maxilla Fused	PERCENT FUSION
CONTROL	6	3	50%
MUTANTS	6	4	66.67%

Figure 17. Graphical representation of the fusion rates of palate shelves in the controls and the *Rdh10* conditional mutants in combo culture. With our preliminary data, we concluded that the RA from controls when grown in the same culture bottles likely rescued the cleft palate seen in mutant maxilla.

Fusion Rate of Maxillary Explant Mono Culture
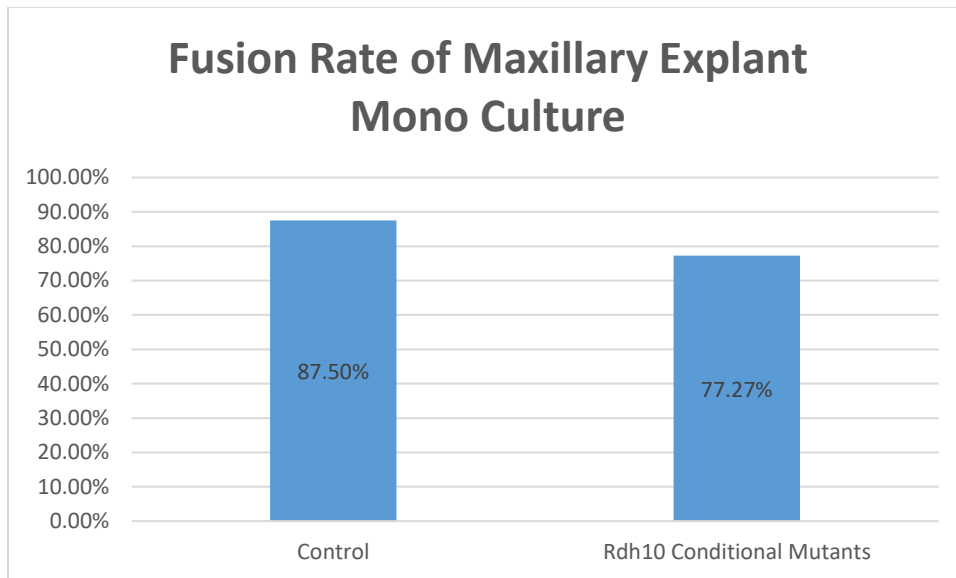
MAXILLARY EXPLANT SINGLE/MONO CULTURE

	Total Maxilla Cultured	Total Maxilla Fused	PERCENT FUSION
CONTROL	16	14	87.50%
MUTANTS	22	17	77.27%

Figure 18.Graphical representation of the fusion rates of palate shelves in the controls and the *Rdh10* conditional mutants obtained in monoculture. Even though it appears that the fusion rate of palate shelves in mutants is fewer than the controls, no statistical difference is observed compared to controls. This data suggests that removal of tongue and the mandible rescues cleft palate in *Rdh10* conditional mutants, suggesting extrinsic role for RA during palate development.
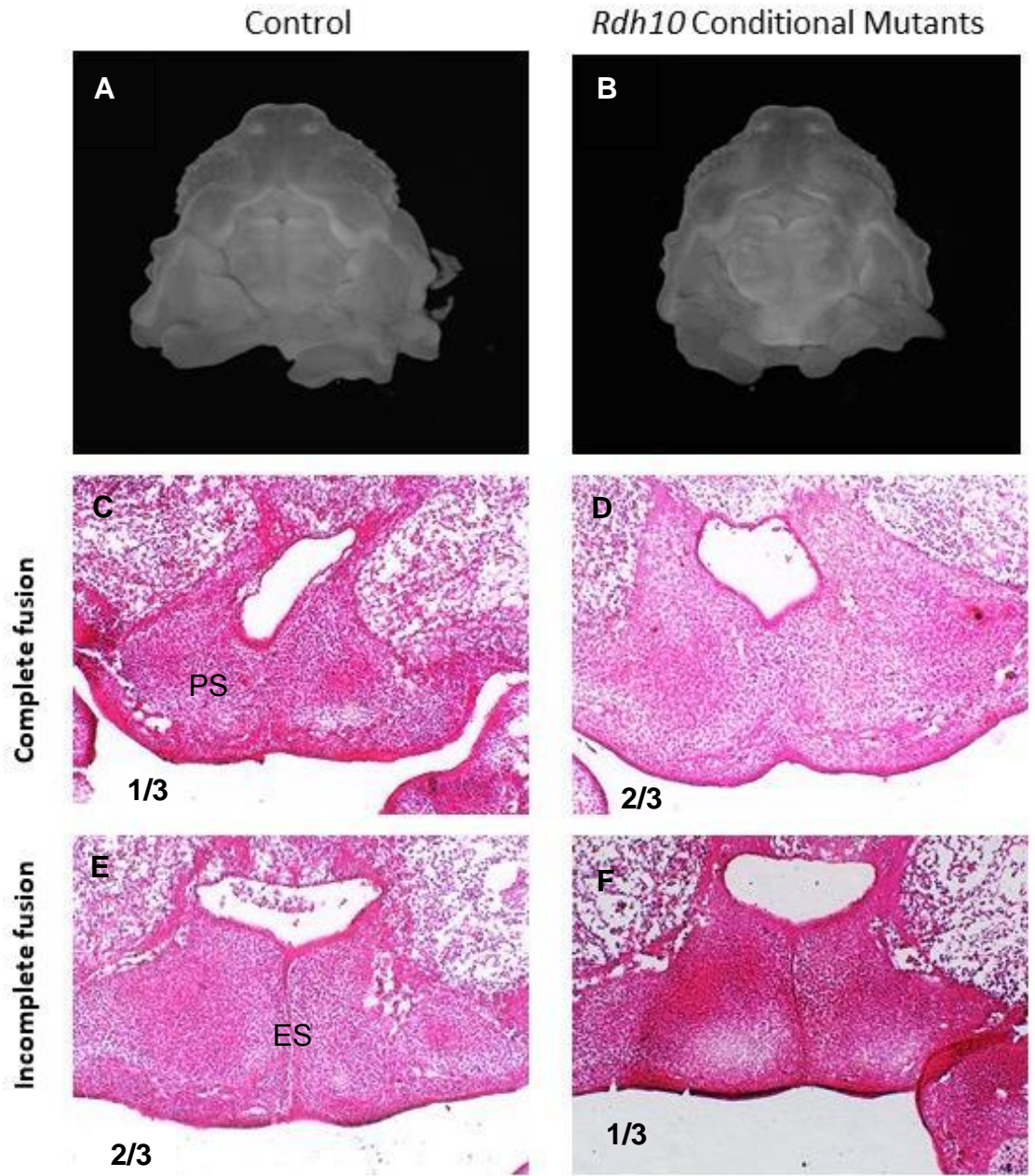
Figure 19.Comparison of histological sections of controls and *Rdh10* conditional mutants after 72 hours in culture. (A) and (B) showing nuclear florescent imaging of the palate shelf. C-F showing histological coronal paraffin sections of the cultured maxilla. Three controls and three mutant samples from three litters were sectioned and stained by hematoxylin and eosin staining. One of the three controls sectioned showed complete fusion (C), two of the mutants showed complete

fusion (D). Two controls showed incomplete fusion (E) in comparison to one mutant that showed incomplete fusion with epithelial seam between the two palate shelves. (F). PS- Palatal Shelf; ES- Epithelial Seam

3.7 Ectopic Fusion in Nasal Region seen in *Rdh10* Conditional Mutants:

Previous studies have shown that *Rdh10* conditional mutants exhibit choanal stenosis or nasal obstruction when we administer tamoxifen at gestational age E7.5(Kurosaka, Wang et al. 2017). The mutants reported in this study were slightly different in breeding. They contained only one pair of *flox* allele while our mutants contain two pair of *flox* allele. Hence, we could expect the kinetics of tamoxifen excision to be slightly different in both cases. We still wanted to see if we see any similar phenotype in our mutants. Hence, we decided to analyze the sections that were stained by hematoxylin and eosin for nasal obstruction. Although not as severe as previously reported by Kurosaka et al, we did observe the nasal obstruction phenotype when we administered tamoxifen at either E7.5 or E8.5. At E12.5, apart from the abnormalities in palate morphology, we also detected a shorter, wider and obliterated sinus opening in two of the three mutants in the SNAZ where RA signaling is seen. Embryos harvested at E13.5 showed an ectopic fusion between the nasal septum and the medial nasal epithelium. 73% of the mutants examined at E13.5 and E14.5 showed this phenotype (Fig 20).

Control | Rdh10 Conditional Mutants
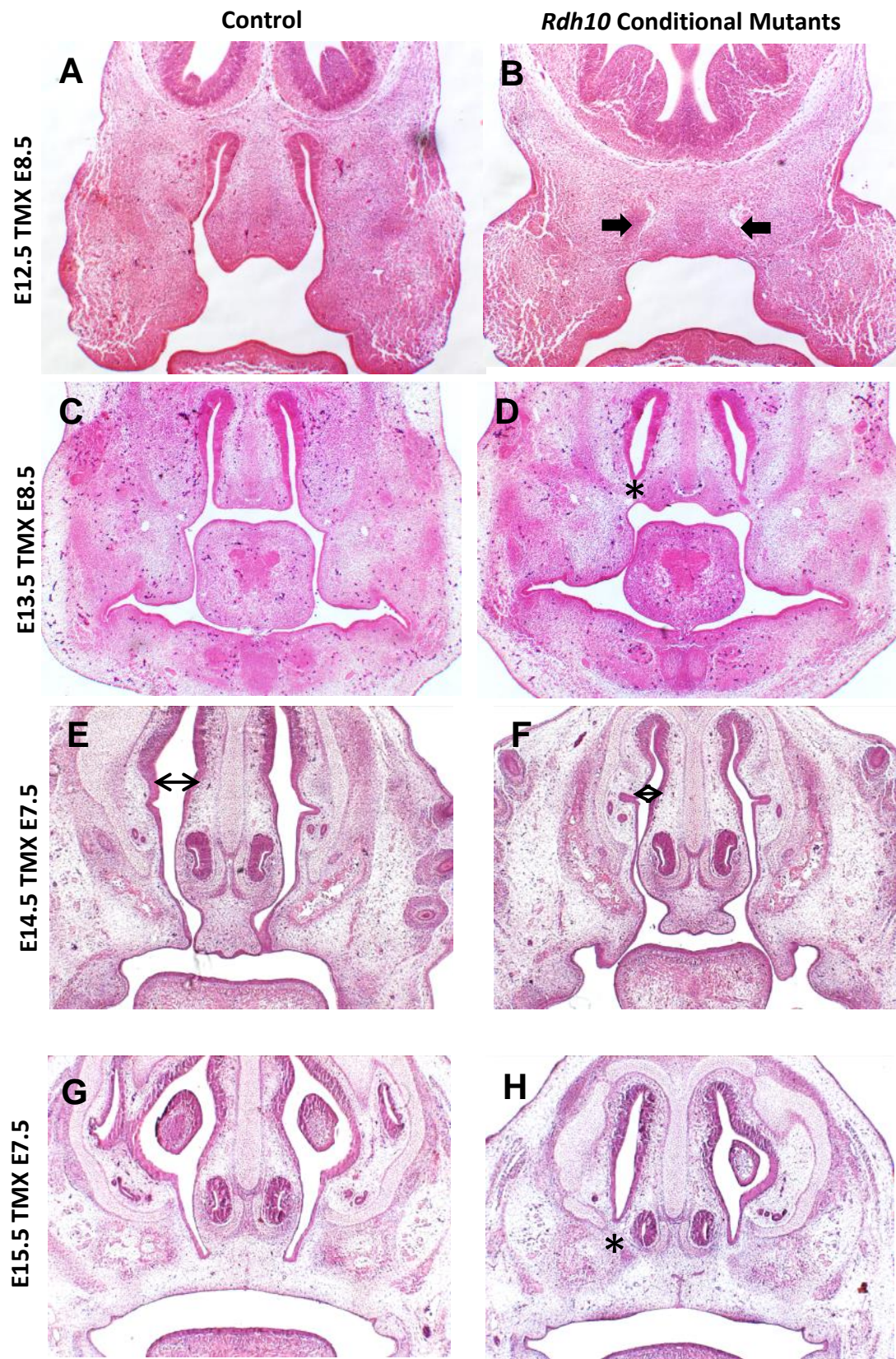
Figure 20.Nasal obstruction and ectopic fusions seen in *Rdh10* conditional mutants. Coronal H &
E sections through the nasal region at stages E12.5, E13.5, E14.5, & E15.5 (A-H). *Rdh10*
conditional mutants show shorter, wider and obliterated sinus at E12.5 (B) compared to controls
(A). At E13.5, controls showed a clear sinus tract(C) while *Rdh10* conditional mutants showed
fusion between the developing nasal sinus and the medial nasal epithelium. At E14.5, mutants
showed obliterated nasal sinus region (F) compared to controls at this stage (E). At E15.5, complete
obliteration of the lower region of the nasal sinus area is seen. Arrows and * depicts regions of
ectopic fusion.

CHAPTER 4: DISCUSSION

The association of cleft palate with lack of Vitamin A/ RA in diet has been known for 80 years now but the mechanisms underlying this defect is unknown. One of the main reasons for the gap in knowledge of how deficient RA affects palate development is due to a lack of a model system to study its function at palate developmental stages. In this study, we have addressed this major gap in knowledge of how RA deficiency affects the development of palate by establishing a model system that will allow us to further investigate the role of RDH10 mediated metabolism of vitamin A in palate development. We did this by inactivating RDH10, a critical enzyme that catalyzes the first step in the conversion of Vitamin A into its active form, RA. We observed 100% of control embryos had fusion of palate shelf at E16.5, while 44% RA deficient mutant embryos had complete cleft of the secondary palate.

In our study, administering tamoxifen at different gestational periods before palate initiation also proved to be useful in understanding the period when endogenous RA is needed for palate development. Administration of tamoxifen at early gestational age E7.5 caused higher percentage of mutant lethality and later stages of administration at E10.5 showed normal phenotype. This observation suggests that RDH10 mediated metabolism of RA maybe needed during a specific time frame at early stages of palate development.

Previous studies show that there is no RA signaling within the developing palate.(Okano, Kimura et al. 2012). However, for the very first time, using RARE-LacZ mice, we have shown RA signaling within the developing palate shelves at embryonic age E12.5. This difference in the result obtained could be due to a variation in the way the experiment was carried out. Removal of the tongue and the mandible allowed better penetration of the X-gal staining and capturing most of the RA activity in the developing palate shelves at E12.5.

The finding that *Rdh10* inactivation causes cleft palate and the presence of RA signaling within the developing palate shelf tissue at E12.5 raised a question of what mechanisms RA regulates in the developing palate. Interestingly, even though we detect RA signaling within palate shelf tissues and an increase in cell proliferation at the bend region in E12.5, the cleft palate seen in RA deficient mutants was not due to an intrinsic defect in the palate shelf itself. Our study demonstrates that the cleft palate seen in RA deficiency is secondary to abnormal tongue and mandible development in *Rdh10* mutants. We have come to this conclusion based on the ex vivo maxillary explant culture experiment and the measurement of tongue height from histological sections at E14.5. Cleft palate seen in *Rdh10* mutants was rescued upon culturing maxilla independent of tongue and mandible.

Our data put together provide us with useful insights on the role on endogenous RA in palate development. Our results demonstrate a predominant non-intrinsic role of endogenous RA in causing cleft palate in *Rdh10* mutants.

In contrast to the gap in knowledge of RA deficient cleft palate, the teratogenic effects of excess RA is well known. From published literature, we know that excess dosage of RA can also cause cleft palate. Comparing the findings of our study of RA deficiency with other published studies on RA excess, it is clear that the mechanisms underlying the two are quite different.

In conclusion, the RA deficient model of cleft palate needs further investigation. The findings from my thesis work further directs our research work to mandibular and tongue abnormalities that may be caused due to RA deficiency. Small mandible, difficulty in respiration due to glossoptosis and cleft palate are features of a serious syndrome called the Pierre Robin Sequence. The primary data obtained in my research work suggest a possibility of RA deficiency resembling the Pierre Robin Sequence. We can confirm this hypothesis by directing future experiments towards identifying defects in mandibular and tongue development.

REFERENCES

1   (1996). "Positional cloning of a gene involved in the pathogenesis of Treacher

      Collins syndrome. The Treacher Collins Syndrome Collaborative Group." Nat Genet

      12(2): 130-136.

2   Benko, S., J. A. Fantes, J. Amiel, D. J. Kleinjan, S. Thomas, J. Ramsay, N. Jamshidi, A.

      Essafi, S. Heaney, C. T. Gordon, D. McBride, C. Golzio, M. Fisher, P. Perry, V.

      Abadie, C. Ayuso, M. Holder-Espinasse, N. Kilpatrick, M. M. Lees, A. Picard, I. K.

      Temple, P. Thomas, M. P. Vazquez, M. Vekemans, H. Roest Crollius, N. D. Hastie, A.

      Munnich, H. C. Etchevers, A. Pelet, P. G. Farlie, D. R. Fitzpatrick and S. Lyonnet

      (2009). "Highly conserved non-coding elements on either side of SOX9 associated

      with Pierre Robin sequence." Nat Genet **41**(3): 359-364.

3   Bi, W., W. Huang, D. J. Whitworth, J. M. Deng, Z. Zhang, R. R. Behringer and B. de

      Crombrugghe (2001). "Haploinsufficiency of Sox9 results in defective cartilage

      primordia and premature skeletal mineralization." Proc Natl Acad Sci U S A **98**(12):

      6698-6703.

4   Bush, J. O. and R. Jiang (2012). "Palatogenesis: morphogenetic and molecular

      mechanisms of secondary palate development." Development **139**(2): 231-243.

5   Canfield, M. A., M. A. Honein, N. Yuskiv, J. Xing, C. T. Mai, J. S. Collins, O. Devine, J.

      Petrini, T. A. Ramadhani, C. A. Hobbs and R. S. Kirby (2006). "National estimates

      and race/ethnic-specific variation of selected birth defects in the United States,

      1999-2001." Birth Defects Res A Clin Mol Teratol **76**(11): 747-756.

6   Centers for Disease Control and Prevention [CDC]. (2014). "Birth Defects. ." Centers for Disease Control and Prevention, from http://www.cdc.gov/ncbddd/birthdefects/index.html.

7   Clagett-Dame, M. and D. Knutson (2011). "Vitamin A in reproduction and development." Nutrients **3**(4): 385-428.

8   Ding, H., X. Wu, H. Bostrom, I. Kim, N. Wong, B. Tsoi, M. O'Rourke, G. Y. Koh, P. Soriano, C. Betsholtz, T. C. Hart, M. L. Marazita, L. L. Field, P. P. Tam and A. Nagy (2004). "A specific requirement for PDGF-C in palate formation and PDGFR-alpha signaling." Nat Genet **36**(10): 1111-1116.

9   Ferguson, M. W. (1988). "Palate development." Development **103 Suppl**: 41-60.

10   Gendron-Maguire, M., M. Mallo, M. Zhang and T. Gridley (1993). "Hoxa-2 mutant mice exhibit homeotic transformation of skeletal elements derived from cranial neural crest." Cell **75**(7): 1317-1331.

11   Gritli-Linde, A. (2007). "Molecular control of secondary palate development." Developmental Biology **301**(2): 309-326.

12   Hu, X., J. Gao, Y. Liao, S. Tang and F. Lu (2013). "Retinoic acid alters the proliferation and survival of the epithelium and mesenchyme and suppresses Wnt/β-catenin signaling in developing cleft palate." Cell Death & Disease **4**(10): e898.

13   Kauffman (1992). The Atlas of Mouse Development. London, Elsevier.

14   Krapels, I. P., I. A. van Rooij, M. C. Ocke, C. E. West, C. M. van der Horst and R. P. Steegers-Theunissen (2004). "Maternal nutritional status and the risk for orofacial cleft offspring in humans." J Nutr **134**(11): 3106-3113.

15   Kurosaka, H., Q. Wang, L. Sandell, T. Yamashiro and P. A. Trainor (2017). "Rdh10 loss-of-function and perturbed retinoid signaling underlies the etiology of choanal atresia." Human Molecular Genetics **26**(7): 1268-1279.

16   Lan, Y., N. Zhang, H. Liu, J. Xu and R. Jiang (2016). "Golgb1 regulates protein glycosylation and is crucial for mammalian palate development." Development (Cambridge, England) **143**(13): 2344-2355.

17   Marazita, M. L. (2002). Genetic Etiologies of Facial Clefting. Understanding Craniofacial Anomalies, John Wiley & Sons, Inc.**:** 147-161.

18   McKinney, C. M., B. Chowchuen, W. Pitiphat, T. Derouen, A. Pisek and K. Godfrey (2013). "Micronutrients and oral clefts: a case-control study." J Dent Res **92**(12): 1089-1094.

19   Metzler, M. A. and L. L. Sandell (2016). "Enzymatic Metabolism of Vitamin A in Developing Vertebrate Embryos." Nutrients **8**(12): 812.

20   Mori-Akiyama, Y., H. Akiyama, D. H. Rowitch and B. de Crombrugghe (2003). "Sox9 is required for determination of the chondrogenic cell lineage in the cranial neural crest." Proc Natl Acad Sci U S A **100**(16): 9360-9365.

21   Okano, J., W. Kimura, V. E. Papaionnou, N. Miura, G. Yamada, K. Shiota and Y. Sakai (2012). "The regulation of endogenous retinoic acid level through CYP26B1 is required for elevation of palatal shelves." Dev Dyn **241**(11): 1744-1756.

22   Okano, J., S. Suzuki and K. Shiota (2007). "Involvement of apoptotic cell death and

cell cycle perturbation in retinoic acid-induced cleft palate in mice." Toxicology and

Applied Pharmacology **221**(1): 42-56.

23   Peter (1924). "Die entwicklung des Säugetiergaumens. Ergeb." Anat.

Entwickl.Gesch. **25**: 448-564.

24   Reardon, W., R. M. Winter, P. Rutland, L. J. Pulleyn, B. M. Jones and S. Malcolm

(1994). "Mutations in the fibroblast growth factor receptor 2 gene cause Crouzon

syndrome." Nat Genet **8**(1): 98-103.

25   Rhinn, M. and P. Dolle (2012). "Retinoic acid signalling during development."

Development **139**(5): 843-858.

26   Sandell, L. L., H. Kurosaka and P. A. Trainor (2012). "Whole mount nuclear

fluorescent imaging: convenient documentation of embryo morphology." Genesis

50(11): 844-850.

27   Sandell, L. L., M. L. Lynn, K. E. Inman, W. McDowell and P. A. Trainor (2012).

"RDH10 oxidation of Vitamin A is a critical control step in synthesis of retinoic acid

during mouse embryogenesis." PLoS One **7**(2): e30698.

28   Sandell, L. L., B. W. Sanderson, G. Moiseyev, T. Johnson, A. Mushegian, K. Young, J.

P. Rey, J. X. Ma, K. Staehling-Hampton and P. A. Trainor (2007). "RDH10 is essential

for synthesis of embryonic retinoic acid and is required for limb, craniofacial, and

organ development." Genes Dev **21**(9): 1113-1124.

29   Shenefelt, R. E. (1972). "Morphogenesis of malformations in hamsters caused by

retinoic acid: relation to dose and stage at treatment." Teratology **5**(1): 103-118.

30   Veau V. Division Palatine., M. a. C. (1931). Veau V. Division Palatine. Paris, Masson

      and Cie

31   Wilcox, A. J., R. T. Lie, K. Solvoll, J. Taylor, D. R. McConnaughey, F. Abyholm, H.

      Vindenes, S. E. Vollset and C. A. Drevon (2007). "Folic acid supplements and risk of

      facial clefts: national population based case-control study." Bmj **334**(7591): 464.

32   Zhang, H., X. Liu, Z. Gao, Z. Li, Z. Yu, J. Yin, Y. Tao and L. Cui (2017). "Excessive

      retinoic acid inhibit mouse embryonic palate mesenchymal cell growth through

      involvement of Smad signaling." Animal Cells and Systems **21**(1): 31-36.

CURRICULUM VITA

Name: Swetha Raja

Address: 2234 S Preston St, Apt 4 Louisville KY, 40217

Date of Birth: 05/05/1993

Education:

- Bachelors of Dental Surgery, Sri Ramachandra University, 2010-2015

- Masters in Oral Biology, University of Louisville, 2016-2017

Professional Societies:

- American Association for Dental Research (AADR), 2015-Present

- International Association of Dental Research (IADR), 2015-Present

- American Dental Association (ADA), 2014- Present

- Indian Dental Association (IDA), 2010- Present